U.S. DEPARTMENT OF COMMERCE
National Bureau of Standards
Washington, D.C. 20234

Date: August 4, 1970

Reply to Attn of: 500.01

Subject: Review and Updating of Information on Transmission and Reflection of Electrons by Aluminum Shields. (Work done under Contract R-80)

To: Mr. Arthur Reetz
Space Vehicles Division, Code RV-1
National Aeronautics and Space Administration
Washington, D. C. 20546

And:

Dr. Nat Edmonson, Jr.
Space Sciences Laboratory
Marshall Space Flight Center, Code R-P-N
Huntsville, Alabama 35812

Summary

This memorandum reviews the available information regarding the transmission and reflection of high-energy electrons by aluminum shields. The incident electron energies considered lie between 0.5 MeV and 10.0 MeV, covering the region of interest for shielding against electrons in natural and artificial radiation belts. Emphasis is placed on summary parameters such as number and energy transmission coefficients, reflection coefficients, and practical ranges. Extensive new data are tabulated which were calculated with the Monte Carlo computer program ETRAN 16. Numerous comparisons are also made with all pertinent experiments in order to review the experimental situation and to verify the validity of the method of calculation.

Martin J. Berger

Martin J. Berger
Center for Radiation Research
Radiation Theory Section

1. Purpose and Scope

This memorandum contains new data pertaining to the transport of electrons through plane-parallel aluminum targets. The data are excerpted from a more detailed manuscript now being prepared for publication in a technical journal. The work was undertaken for two purposes: (a) to make comparisons between calculated and experimental electron transport data, and (b) to provide information needed for engineering estimates of protection against space radiation. The theoretical results have been obtained with the Monte Carlo computer program ETRAN[1-3].

The data in this memorandum are for incident electron beams with various energies between 0.25 MeV and 10.0 MeV, and include (a) number and energy reflection coefficients, (b) number and energy transmission coefficients, and (c) practical ranges. Information has also been obtained by the energy deposited as a function of the depth in the target, which will be presented in a later report.

The transmission and reflection coefficients in this memorandum are an updating and extension of earlier data[2]. The previous results, limited to target thicknesses no greater than 70% of the mean range of the incident electrons, were obtained with Version 5 of ETRAN in which no allowance was made for the transport of secondary electrons. This deficiency has been remedied in Verion 16 of ETRAN which was used in the present work. The earlier data were used by Ingley[4] to estimate radiation doses in space vehicles. As he pointed out, there are situations of practical interest where one needs to know the transmission of electrons through shields greater than 70% of the range. The present tabulations were therefore extended to target thicknesses equal to 100% of the range.

It is not always easy to justify on a purely logical basis, and to understand the consequences of, the various approximations that enter into a Monte Carlo model such as that used for ETRAN. Moreover, even though the cross sections for the interactions between electrons, photons, and atoms are on the whole well known for the materials and energies of interest,

some uncertainties remain, e.g., in respect to the production of bremsstrahlung. It is therefore desirable to test the adequacy of the Monte Carlo model and of the cross sections simultaneously, through comparison with electron transport experiments. The argument can also be reversed and the transport calculations can be used as a means of checking the reliability of various experiments and the consistency between them. Once an adequate body of mutually supporting theoretical and experimental evidence has been accumulated, a program such as ETRAN can be used with confidence for getting systematic solutions to a large class of problems.

Various comparisons between the predictions of ETRAN and experimental data have already been made[1,2,5-14]. In the present memorandum, additional evidence is collected regarding reflection and transmission coefficients, covering ground not covered previously in the literature.

2. Assumed Initial Conditions and Target Configuration

Recently, new versions of ETRAN have been developed which can be used to treat three-dimensional target configurations. However, in the present memorandum the discussion is limited to problems that can be described using only a single spatial variable. The target is thus assumed to be a plane-parallel slab of finite thickness in the z-direction and effectively unbounded (i.e., large compared to an electron range) in the x- and y-directions.

Transmission and reflection coefficients are considered as functions of the target thickness z, of the incident electron kinetic energy T_0, and the incident obliquity θ_0. This angle is defined as the angle between the incident electron velocity vector and the normal to the target surface, and goes from 0° (perpendicular incidence) to 90° (grazing incidence). Results are presented not only for specific values of θ_0, but also for an assumed incident electron flux isotropic over one hemisphere, i.e., with equal numbers of electrons crossing a unit area of surface perpendicular to the incident velocity vector for all θ_0 between 0° and 90°. With an incident isotropic flux, the corresponding electron current across a unit area of

the target surface has an angular distribution proportional to cos θ_o. Such a cosine-law source is a useful approximation in space shielding studies, in conditions where the actual angular distribution of the incident electrons is not well known.

3. Scaling

The explicit dependence of the transmission coefficients on the incident electron energy T_o can be greatly reduced by scaling. For this purpose, the transmission coefficients are tabulated as functions of the ratio z/r_o, where z is the actual target thickness and r_o is the mean range of the incident electrons. The mean range is understood to be the rectified pathlength (also called c.s.d.a. range) computed in the continuous-slowing-down-approximation according to the equation

$$r_o(T_o) = \int_o^{T_o} dT/L(T),$$

where L(T) is the mean energy loss per unit pathlength. A short list of r_o-values of aluminum is given in Table 1.

4. Reflection Coefficients

Two summary parameters will be used to describe the current of reflected electrons: (a) the number reflection coefficient R_N, also called the number albedo, which is defined to be the average number of reflected electrons per incident electron; (b) the energy reflection coefficient R_E, also called the energy albedo, which is defined as the average amount of reflected electron energy per unit incident energy. Contributions to the reflection coefficients are made not only by primary electrons but also by secondary electrons that have been produced in electron-electron collisions or by the absorption of secondary bremsstrahlung photons. The reflection coefficients increase with target thickness until saturation is reached at a target thickness equal to half the range r_o or smaller. Many of the results given here are for targets with saturation thickness.

Fig. 1 shows the number reflection coefficient R_N for electrons incident perpendicularly on aluminum targets of saturation thickness. Experimental results from a large number of publications[15-30] are plotted vs the incident electron energy T_o (from 0.06 MeV to 12.0 MeV) and are compared with a calculated curve (with an estimated statistical uncertainty of 5% or less). There are considerable discrepancies between the results of some of the experiments, indicating perhaps that the determination of the relatively small reflection coefficients is not an easy matter. For a discussion of possible reasons for some of the discrepancies, see, e.g., Tabata[19].

The number reflection coefficient is shown in Fig. 2 as function of the incident obliquity angle θ_o; the agreement with experiment[15,19,20,31] is good. Satisfactory agreement is also found with the available experimental data[24,25] on the energy reflection coefficient, as shown in Fig. 3.

Table 2 gives calculated values of the number reflection coefficient R_N and the energy reflection coefficient R_E for many target thicknesses, for incident angles $\theta_o = 0^o, 30^o, 45^o, 60^o, 75^o$, and 89^o, and for incident energies $T_o = 1$ MeV and 6 MeV. It can be seen that R_N increases strongly with θ_o; in fact, for $T_o = 6.0$ MeV, the value of R_N for $\theta_o = 89^o$ becomes as large as 1.03. A careful examination of the calculation, and additional numerical experimentation, have indicated that this large value of R_N is not a statistical fluke but results from the contribution of a large number of secondary electrons produced by the absorption of secondary bremsstrahlung.

Table 3 gives values of R_N and R_E for cosine-law sources, for incident energies $T_o = 0.5, 1.0, 2.0, 4.0, 6.0, 8.0$ and 10.0 MeV. The reflection coefficients are slowly varying functions of the incident electron energy, decreasing with T_o until at energies near 10 MeV there is a leveling off because of the increasing contribution of bremsstrahlung-produced secondary electrons. The statistical uncertainty of the number reflection coefficients, i.e., the standard deviation σ_N, is indicated in Tables 2 and 3. The standard deviation of the energy reflection coefficients σ_E, for

corresponding conditions is approximately equal to $2 \frac{R_E}{R_N} \sigma_N$.

5. Transmission Coefficients

The summary parameters of interest are: (a) the number transmission coefficient T_N, which is defined as the average number of transmitted electrons per incident electron; (b) the energy transmission coefficient T_E, which is defined as the average amount of electron energy transmitted per unit incident energy.

Each transmitted particle, be it a primary electron or secondary electron, can make a contribution to the transmission coefficient. In fact, T_N (but not T_E) becomes greater than unity for a thin target; there is charge depletion in the target due to the escape of secondary electrons.

The above definition of the transmission coefficient T_N corresponds to the most common case in which the transmitted charge is measured, e.g., with a Faraday cup. Other experimental arrangements are also used which differ in regard to the treatment of events in which several associated particles emerge together from the target (a primary electron accompanied by one or more secondary electrons, or two or more secondary electrons which are descendants of the same primary electron). 2π- counters have been used which record such events as a single differential in angle pulse. Sometimes the emerging electron current is obtained with a detector covering only a small solid angle, and the transmission coefficient is then obtained by integration over a 2π- solid angle. With such an arrangement, the detector can only record one of a group of simultaneously emerging electrons. Slight adjustments in the scoring procedure in the ETRAN program are possible by which the transmission coefficient appropriate to a given experimental arrangement can be computed.

In Figs. 4a-h, calculated number transmission coefficients T_N for the case of perpendicular incidence are compared with the results of various experiments[15-18,23,32,33] at eight energies between 0.25 MeV and 10 MeV. The calculated results are based on samples of 10,000 Monte Carlo

histories at each source energy, and the standard deviation of T_N is therefore $\sqrt{T_N(1 - T_N)}/100$. The overall agreement between experiment and calculation is good, and the discrepancies are frequently smaller than those between different experiments. Nevertheless a better understanding of the discrepancies would be desirable. Within the combined experimental and calculational uncertainties, there is good agreement at energies between 0.5 MeV and 3 MeV. At 0.25 MeV the agreement is somewhat less good; in part this may be due to inadequacies of the cross section input at low energies (approximate treatment of atomic binding effects, disregard of microcrystalline nature of medium). At 4 MeV, there is more pronounced discrepancy. At 10 MeV, there is again improved agreement.

The shape of the calculated transmission curve and the experimental transmission curve from Ref. 16 at 4.0 MeV are quite similar, but the curves appear to be displaced with respect to each other. Very close agreement could be obtained if the source energy were 7% to 8% lower than the nominal value. Dr. Ebert has indicated in private correspondence that such an energy shift with respect to the nominal 4.0-MeV value is unlikely to have occurred but cannot be ruled out. In the initial stages of his experiment there were some difficulties in regard to the determination of the beam energy, particularly between 4 and 6 MeV, but he thought that these difficulties had been resolved. It is difficult to understand why ETRAN would make correct predictions at 3 MeV, as is the case, but not at 4 MeV. There is also evidence from other experiments on charge deposition and practical range, discussed in Sections 7 and 8, which supports the validity of the ETRAN results at 4 MeV.

In Fig. 5, experimental[15] and calculated transmission curves are compared for an incident obliquity angle $\theta_0 = 45^\circ$ and incident energies between 0.25 MeV and 1.0 MeV; the agreement is good. In Fig. 6, transmission curves are given for perpendicular incidence and an incident energy of 10.0 MeV for various media including Be, C, Al, Cu, Ag, and Pb. Satisfactory agreement is found with corresponding experimental results[16,34].

Table 4 gives calculated values of the number transmission coefficient T_N and of the energy transmission coefficient T_E for many target thicknesses and for incident directions $\theta_o = 0^o, 30^o, 45^o, 60^o, 75^o$, and 89^o, for $T_o = 1.0$ MeV and 6.0 MeV. Table 5 gives T_N and T_E for cosine-law sources and incident energies of $T_o = 0.5$, 1.0, 2.0, 4.0, 6.0, 8.0, and 10.0 MeV. The standard deviation σ_N of results for T_N is given. The corresponding standard deviation σ_E of T_E is estimated to be $2 \frac{T_E}{T_N} \sigma_N$. Inspection of Table 5 confirms the effectiveness of scaling through use of the thickness variable z/r_o, the residual energy dependence being rather small so that interpolation with respect to source energy is easy.

6. Transmission of Bremsstrahlung Energy

In the course of traversing the target, the electrons produce bremsstrahlung. The mean free path of the bremsstrahlung photons is large compared to the electron range, so that a significant amount of energy can escape from the target in the form of bremsstrahlung, even when the target is thick enough to stop all primary electrons. The energy transmission in the form of bremsstrahlung is usually characterized in terms of the bremsstrahlung efficiency Y. This quantity is defined, in the present context, as the fraction of the incident electron kinetic energy that emerges as bremsstrahlung energy through the transmission face of the target. The efficiency begins to be appreciable at incident energies of several MeV. Supplementing earlier efficiency data for perpendicular electron incidence[5] and for a cosine-law source[2,14], Fig. 7 shows the dependence of Y on the electron incident obliquity angle θ_o, for 6.0 MeV electrons incident on aluminum targets. It can be seen that the efficiency lies between 1 and 4%, depending on the target thickness and incident electron direction.

7. Charge Deposition Distributions

Those electrons which are not reflected or transmitted come to rest in the target and deposit their charge at various depths. The distribution of deposited electric charge with depth, $D_c(z)$, is closely related to the transmission curve $T_N(z)$. In fact, except for a backscattering correction,

$D_c(z)$ is equal to the derivative of the transmission curve with respect to z. The ETRAN program has the capability of extracting from the same set of sampled Monte Carlo histories not only the transmission coefficients but also the charge deposition distributions. Experimental data on the charge deposition distribution are available[35,36]. It is therefore pertinent to make comparisons which can provide a sensitive test of the Monte Carlo treatment of the electron transport problem.

Comparisons with experimental charge deposition distributions are made in Figs. 8a-g for various media. In some cases the incident electron energy in the experiment differed slightly from that assumed in the calculation, but this difficulty was circumvented by plotting the charge deposition distribution vs the ratio z/r_o. It should also be mentioned that the experimental data are in all cases for semi-infinite media whereas the calculations are semi-infinite Be and Al media, for slab targets with thicknesses equal to $0.8r_o$, and $0.6r_o$ for Cu, Ag, and Pb, respectively. The calculated distributions for Cu, Ag, and Pb therefore are somewhat lower than the experimental distributions near the transmission face of target, as is to be expected. Elsewhere, there is generally good agreement. The peak position of the charge distribution is predicted correctly, as is the charge depletion at shallow depths. The results include the case of 4.0 MeV electrons incident on aluminum, and the agreement with experiment obtained in this case lends support to the view that the calculated transmission curve in Fig. 4g is also correct.

8. Practical Ranges

Another useful parameter characterizing the transmission of electrons through plane-parallel targets is the practical range r_p (also called the extrapolated range[37]). This quantity is determined by extrapolating the approximately linear middle portion of the transmission curve $T_N(z)$; r_p is taken to be equal to the value of z for which the extrapolated linear transmission curve reaches the value zero.

An analysis of the calculated transmission curves for perpendicular incidence given in this memorandum leads to an empirical formula

$$r_p = 0.548\ T_o - 0.155\ g/cm^2\ Al$$

$$1\ MeV \lesssim T_o \lesssim 12\ MeV$$

which is rather close to an earlier empirical formula in this energy region,

$$r_p = 0.530\ T_o - 0.106\ g/cm^2\ Al$$

$$1\ MeV \lesssim T_o \lesssim 20\ MeV$$

derived by Katz and Penfold[38] from the experimental data available in 1951.

A sensitive way of comparing calculated and experimental practical range-values is provided by plotting the quantity r_p/T_o *vs* T_o. This is done in Fig. 9 over the energy interval from 0.25 MeV to 12 MeV. It can be seen that the Monte Carlo results and Katz-Penfold results differ little from each other, and are in agreement with all experimental results[15,17,23,32,33,39] except those from Ref. 16 which appear to have a different energy dependence.

9. References

1. M. J. Berger, Methods in Computational Physics, Vol. 1, pp. 135-215, Academic Press, N. Y., 1963.
2. M. J. Berger and S. M. Seltzer, Protection Against Space Radiation, pp. 285-322, NASA Report SP-169, 1968.
3. M. J. Berger and S. M. Seltzer, NBS Reports 9836 and 9837, 1968.
4. J. S. Ingley, Bellcom, Inc., Memorandum TM 68-1011-3, August 23, 1968.
5. M. J. Berger and S. M. Seltzer, Second Symposium on Protection Against Radiations in Space, pp. 437-448, NASA Report SP-71, 1964.
6. M. J. Berger and S. M. Seltzer, Ann. New York Academy of Sciences, 161. 8-23 (1969).
7. M. J. Berger and S. M. Seltzer, Second International Conference on Accelerator Dosimetry and Experience, pp. 302-322, US AEC Report CONF-691101, 1969.
8. M. J. Berger and S. M. Seltzer, J. Atmosph. and Terr. Physics 32, 1015-1045 (1970).
9. M. J. Berger and S. M. Seltzer, Phys. Rev. July 1970, in press.
10. M. J. Berger, S. M. Seltzer, S. E. Chappell, J. C. Humphreys, and J. W. Motz, Nucl. Instr. Methods 69, 181-193 (1969).
11. R. C. McCall, W. R. Nelson, J. M. Wyckoff, and J. S. Pruitt, Second International Conference on Accelerator Dosimetry and Experience, pp. 684-691, US AEC Report CONF-691101, 1969.
12. W. L. McLaughlin and E. K. Hussmann, pp. 579-590, International Atomic Energy Agency Report IAEA-SM-23/43 (1969).
13. J. A. Lonergan, C. P. Jupiter and G. Merkel, J. Appl. Physics 41, 678-688 (1970).
14. D. H. Rester, W. E. Dance, and J. H. Derrickson, J. Appl. Phys. 41, 2682 (1970).
15. W. E. Miller and H. D. Hendricks, NASA Technical Note TN D-4363 (1968).
16. P. J. Ebert, A. F. Lauzon, and E. M. Lent, Phys. Rev. 183, 422 (1969); also UCRL-71462 (1968).

17. B.N.C. Agu, T. Burdett, and E. Matsukawa, Proc. Phys. Soc. (London) 71, 201 (1958).
18. Y. Nakai, K. Matsuda, T. Takagaki, and K. Kimura, Ann. Rep. Jap. Assoc. Rad. Res. on Polymers 5, 7 (1964).
19. T. Tabata, Phys. Rev. 162, 336 (1967).
20. A. J. Cohen and K. F. Koral, NASA Technical Note TN D-2782 (1965).
21. J. Saldick and A. O. Allen, J. Chem. Phys. 22, 438 (1954).
22. J. Jakschik and K. P. Jüngst, Nucl. Instr. Methods 79, 240-244 (1970).
23. W. E. Miller, NASA Technical Note TN D-5724 (1970).
24. D. H. Rester, W. J. Rainwater, Jr., and J. H. Johnson. Private communication, 1964.
25. K. A. Wright and J. G. Trump, J. Appl. Phys. 33, 687 (1962).
26. H. Frank, Z. Naturforsch. 14a, 247 (1959).
27. R. W. Dressel, Phys. Rev. 144, 332 (1966).
28. D. Harder and H. Ferbert, Phys. Letters 9, 233 (1964).
29. P. Ya. Glazunov and V. G. Guglya, Dokl. Adad. Nauk. SSSR 159, 632 (1964).
30. J. G. Trump and R. J. Van de Graaff, J. Appl. Phys. 18, 327-332 (1947).
31. S. Okabe, T. Tabata, and R. Ito, Ann. Report Rad. Center of Osaka Prefecture, 4, 50 (1963); 6, 51 (1965).
32. H. H. Seliger, Phys. Rev. 100, 1029 (1955).
33. D. Harder and G. Poschet, Phys. Letters 24B, 519 (1967).
34. D. Harder, Habilitationsschrift, University of Wurzburg, 1965.
35. B. Gross and K. A. Wright, Phys. Rev. 114, 725 (1959).
36. T. Tabata, R. Ito, and S. Okabe, Ann. Report of the Rad. Center of Osaka Prefecture, 9, 34-39 (1968); also private communication and paper submitted to Phys. Rev.
37. R. D. Evans, The Atomic Nucleus, p. 623, McGraw-Hill, New York, 1955.
38. L. Katz and A. S. Penfold, Rev. Mod. Phys. 24, 28-44 (1952).
39. S. Horikiri, Y. Nakai, H. Iomo, and K. Matsuda, Paper given at Jap. Phys. Soc. Annual Meeting (1959). AEC-tr-6231.

Table 1. Electron c.s.d.a. range in aluminum.

T_0 (MeV)	r_0 (g/cm^2)	T_0 (MeV)	r_0 (g/cm^2)
0.25	0.082	2.5	1.54
0.4	0.164	3.0	1.86
0.5	0.224	3.5	2.17
0.6	0.287	4.0	2.48
0.8	0.417	4.5	2.78
0.9	0.483	5.0	3.08
1.0	0.549	5.5	3.37
1.2	0.683	6.0	3.66
1.4	0.816	7.0	4.23
1.6	0.949	8.0	4.78
1.8	1.08	9.0	5.32
2.0	1.21	10.0	5.84

Table 2. Reflection of electrons by plane-parallel aluminum targets. Electrons are assumed to be incident on a target of thickness z with kinetic energy T_o and with various obliquity angles between 0° (perpendicular incidence) and 89° (grazing incidence).

(a) Percentage number reflection, 100 R_N; T_o = 1.0 MeV.

z/r_o	$\theta_o = 0^\circ$	30°	45°	60°	75°	89°
0.05	0.4±0.1	1.0±0.1	3.0±0.2	12.5±0.3	36.9±0.5	80.9±0.6
0.10	1.1 0.1	3.5 0.2	9.5 0.3	23.0 0.4	45.4 0.5	84.4 0.6
0.15	3.0 0.2	6.9 0.3	14.8 0.4	28.7 0.5	50.0 0.6	86.4 0.6
0.20	5.2 0.2	10.1 0.3	18.5 0.4	31.8 0.5	51.9 0.6	87.2 0.5
0.25	7.2 0.3	11.9 0.3	20.3 0.4	33.1 0.5	52.6 0.6	87.4 0.5
0.30	8.5 0.3	13.1 0.3	21.0 0.4	33.5 0.5	52.8 0.6	87.5 0.5
0.35	8.9 0.3	13.4 0.3	21.2 0.4	33.5 0.5	52.8 0.6	87.6 0.5
0.40	9.0 0.3	13.5 0.3	21.2 0.4	33.6 0.5	52.8 0.6	87.6 0.5
0.45	9.0 0.3	13.5 0.3	21.2 0.4	33.6 0.5	52.8 0.6	87.6 0.5
0.50	9.0 0.3	13.5 0.3	21.2 0.4	33.6 0.5	52.8 0.6	87.6 0.5
0.55	9.0 0.3	13.5 0.3	21.2 0.4	33.6 0.5	52.8 0.6	87.6 0.5
0.60	9.0 0.3	13.5 0.3	21.2 0.4	33.6 0.5	52.8 0.6	87.6 0.5
0.65	9.0 0.3	13.5 0.3	21.2 0.4	33.6 0.5	52.8 0.6	87.6 0.5
0.70	9.0 0.3	13.5 0.3	21.2 0.4	33.6 0.5	52.8 0.6	87.6 0.5
0.75	9.0 0.3	13.5 0.3	21.2 0.4	33.6 0.5	52.8 0.6	87.6 0.5
0.80	9.0 0.3	13.5 0.3	21.2 0.4	33.6 0.5	52.8 0.6	87.6 0.5
0.85	9.0 0.3	13.5 0.3	21.2 0.4	33.6 0.5	52.8 0.6	87.6 0.5
0.90	9.0 0.3	13.5 0.3	21.2 0.4	33.6 0.5	52.8 0.6	87.6 0.5
0.95	9.0 0.3	13.5 0.3	21.2 0.4	33.6 0.5	52.8 0.6	87.6 0.5
1.00	9.0 0.3	13.5 0.3	21.2 0.4	33.6 0.5	52.8 0.6	87.6 0.5

Table 2. (Continued)

(b) Percentage number reflection, 100 R_N; T_o = 6.0 MeV.

z/r_o	θ_o= 0°	30°	45°	60°	75°	89°
0.05	0.6±0.1	0.9±0.1	1.6±0.1	6.2±0.3	30.8±0.5	97.8±0.8
0.10	0.8 0.1	1.3 0.1	3.4 0.2	13.4 0.4	41.3 0.6	101.6 0.7
0.15	0.9 0.1	1.8 0.1	6.2 0.2	18.3 0.4	46.0 0.6	102.9 0.7
0.20	1.3 0.1	3.0 0.2	8.4 0.3	21.0 0.4	48.0 0.6	103.4 0.7
0.25	1.7 0.1	4.1 0.2	9.8 0.3	22.0 0.4	48.5 0.6	103.5 0.7
0.30	1.9 0.1	4.6 0.2	10.2 0.3	22.3 0.4	48.6 0.6	103.5 0.7
0.35	2.1 0.1	4.9 0.2	10.4 0.3	22.4 0.4	48.6 0.6	103.5 0.7
0.40	2.2 0.1	5.0 0.2	10.4 0.3	22.4 0.4	48.6 0.6	103.5 0.7
0.45	2.2 0.1	5.0 0.2	10.4 0.3	22.4 0.5	48.6 0.6	103.5 0.7
0.50	2.2 0.1	5.0 0.2	10.4 0.3	22.4 0.5	48.6 0.6	103.5 0.7
0.55	2.2 0.1	5.0 0.2	10.4 0.3	22.4 0.5	48.6 0.6	103.5 0.7
0.60	2.2 0.1	5.0 0.2	10.4 0.3	22.4 0.5	48.7 0.6	103.5 0.7
0.65	2.2 0.1	5.0 0.2	10.4 0.3	22.4 0.5	48.7 0.6	103.5 0.7
0.70	2.2 0.1	5.0 0.2	10.4 0.3	22.4 0.5	48.7 0.6	103.5 0.7
0.75	2.2 0.1	5.0 0.2	10.4 0.3	22.4 0.5	48.7 0.6	103.5 0.7
0.80	2.2 0.1	5.0 0.2	10.4 0.3	22.4 0.5	48.7 0.6	103.5 0.7
0.85	2.2 0.1	5.0 0.2	10.4 0.3	22.4 0.5	48.7 0.6	103.5 0.7
0.90	2.2 0.1	5.0 0.2	10.4 0.3	22.4 0.5	48.7 0.6	103.5 0.7
0.95	2.2 0.1	5.0 0.2	10.4 0.3	22.4 0.5	48.7 0.6	103.5 0.7
1.00	2.2 0.1	5.0 0.2	10.4 0.3	22.4 0.5	48.7 0.6	103.5 0.7

Table 2. (Continued)

(c) Percentage energy reflection, 100 R_E; T_o = 1.0 MeV.

z/r_o	θ_o= 0°	30°	45°	60°	75°	89°
0.05	0.2	0.5	1.9	9.0	28.3	67.4
0.10	0.6	2.1	5.9	15.3	33.1	69.4
0.15	1.6	3.9	8.5	17.9	35.0	70.2
0.20	2.6	5.3	10.0	19.0	35.7	70.5
0.25	3.3	5.9	10.7	19.4	35.9	70.5
0.30	3.7	6.3	10.9	19.5	35.9	70.6
0.35	3.8	6.3	10.9	19.6	35.9	70.6
0.40	3.8	6.4	10.9	19.6	35.9	70.6
0.45	3.8	6.4	10.9	19.6	35.9	70.6
0.50	3.8	6.4	10.9	19.6	35.9	70.6
0.55	3.8	6.4	10.9	19.6	35.9	70.6
0.60	3.8	6.4	10.9	19.6	35.9	70.6
0.65	3.8	6.4	10.9	19.6	35.9	70.6
0.70	3.8	6.4	10.9	19.6	35.9	70.6
0.75	3.8	6.4	10.9	19.6	35.9	70.6
0.80	3.8	6.4	10.9	19.6	35.9	70.6
0.85	3.8	6.4	10.9	19.6	35.9	70.6
0.90	3.8	6.4	10.9	19.6	35.9	70.6
0.95	3.8	6.4	10.9	19.6	35.9	70.6
1.00	3.8	6.4	10.9	19.6	35.9	70.6

Table 3. Reflection of electrons by plane-parallel aluminum targets. Electrons are assumed to be incident on a target of thickness z with a cosine-law distribution of angles of incidence and with various kinetic energies T_o between 0.5 MeV and 10.0 MeV.

(a) Percentage number reflection, 100 R_N.

z/r_o	T_o= 0.5	1.0	2.0	4.0	6.0	8.0	10.0 MeV
0.05	9.9±0.3	9.8±0.3	9.4±0.3	7.9±0.3	7.9±0.3	6.9±0.3	6.9±0.3
0.10	17.1 0.4	15.6 0.4	15.6 0.4	12.2 0.3	11.3 0.3	10.1 0.3	10.4 0.3
0.15	21.9 0.4	20.2 0.4	19.9 0.4	15.3 0.4	14.0 0.4	12.1 0.3	12.5 0.4
0.20	25.0 0.4	22.9 0.4	22.7 0.4	17.4 0.4	15.6 0.4	13.7 0.4	13.8 0.4
0.25	26.7 0.5	24.5 0.4	24.5 0.4	18.6 0.4	16.4 0.4	14.5 0.4	14.6 0.4
0.30	27.4 0.5	25.2 0.4	25.1 0.5	19.1 0.4	16.8 0.4	14.8 0.4	14.9 0.4
0.35	27.6 0.5	25.4 0.4	25.3 0.5	19.3 0.4	16.9 0.4	15.0 0.4	15.1 0.4
0.40	27.7 0.5	25.4 0.4	25.4 0.5	19.3 0.4	17.0 0.4	15.0 0.4	15.1 0.4
0.45	27.7 0.5	25.4 0.4	25.4 0.5	19.3 0.4	17.0 0.4	15.0 0.4	15.1 0.4
0.50	27.7 0.5	25.4 0.4	25.4 0.5	19.3 0.4	17.0 0.4	15.0 0.4	15.1 0.4
0.55	27.7 0.5	25.4 0.4	25.4 0.5	19.3 0.4	17.0 0.4	15.0 0.4	15.1 0.4
0.60	27.7 0.5	25.4 0.4	25.4 0.5	19.3 0.4	17.0 0.4	15.0 0.4	15.1 0.4
0.65	27.7 0.5	25.4 0.5	25.4 0.5	19.3 0.4	17.0 0.4	15.0 0.4	15.1 0.4
0.70	27.7 0.5	25.4 0.5	25.4 0.5	19.3 0.4	17.0 0.4	15.0 0.4	15.1 0.4
0.75	27.7 0.5	25.4 0.5	25.4 0.5	19.3 0.4	17.0 0.4	15.0 0.4	15.1 0.4
0.80	27.7 0.5	25.4 0.5	25.4 0.5	19.3 0.4	17.0 0.4	15.0 0.4	15.1 0.4
0.85	27.7 0.5	25.4 0.5	25.4 0.5	19.3 0.4	17.0 0.4	15.0 0.4	15.1 0.4
0.90	27.7 0.5	25.4 0.5	25.4 0.5	19.3 0.4	17.0 0.4	15.0 0.4	15.1 0.4
0.95	27.7 0.5	25.4 0.5	25.4 0.5	19.3 0.4	17.0 0.4	15.0 0.4	15.1 0.4
1.00	27.7 0.5	25.4 0.5	25.4 0.5	19.3 0.4	17.0 0.4	15.0 0.4	15.1 0.4

Table 3. (Continued)

(b) Percentage energy reflection, 100 R_E.

z/r_o	T_o= 0.5	1.0	2.0	4.0	6.0	8.0	10.0 MeV
0.05	7.8	7.3	6.5	4.7	3.9	3.2	3.0
0.10	12.5	10.9	9.9	6.7	5.4	4.4	4.3
0.15	15.1	13.0	11.8	7.9	6.3	5.0	4.8
0.20	16.4	14.1	12.7	8.4	6.7	5.4	5.1
0.25	17.0	14.6	13.2	8.7	6.9	5.5	5.3
0.30	17.3	14.7	13.3	8.9	6.9	5.6	5.3
0.35	17.3	14.8	13.4	8.9	6.9	5.6	5.3
0.40	17.3	14.8	13.4	8.9	6.9	5.6	5.3
0.45	17.3	14.8	13.4	8.9	6.9	5.6	5.3
0.50	17.3	14.8	13.4	8.9	6.9	5.6	5.3
0.55	17.3	14.8	13.4	8.9	6.9	5.6	5.3
0.60	17.3	14.8	13.4	8.9	6.9	5.6	5.3
0.65	17.3	14.8	13.4	8.9	6.9	5.6	5.3
0.70	17.3	14.8	13.4	8.9	6.9	5.6	5.3
0.75	17.3	14.8	13.4	8.9	6.9	5.6	5.3
0.80	17.3	14.8	13.4	8.9	6.9	5.6	5.3
0.85	17.3	14.8	13.4	8.9	6.9	5.6	5.3
0.90	17.3	14.8	13.4	8.9	6.9	5.6	5.3
0.95	17.3	14.8	13.4	8.9	6.9	5.6	5.3
1.00	17.3	14.8	13.4	8.9	6.9	5.6	5.3

Table 4. Transmission of electrons by plane-parallel aluminum targets. Electrons are assumed to be incident on a target of thickness z with kinetic energy T_0 and with various obliquity angles between 0° (perpendicular incidence) and 89° (grazing incidence).

(a) Percentage number transmission, 100 T_N; T_0= 1.0 MeV.

z/r_0	θ_0= 0°	30°	45°	60°	75°	89°
0.05	101.1±0.1	100.9±0.1	99.5±0.2	91.5±0.4	69.0±0.5	29.4±0.5
0.10	100.9 0.2	99.0 0.2	93.6 0.3	81.0 0.4	59.6 0.5	25.4 0.4
0.15	98.9 0.2	94.8 0.3	86.8 0.4	73.0 0.5	52.3 0.5	22.1 0.4
0.20	95.6 0.3	89.2 0.4	79.5 0.4	65.0 0.5	46.0 0.5	19.5 0.4
0.25	90.5 0.4	82.6 0.4	71.6 0.5	57.3 0.5	39.8 0.5	16.5 0.4
0.30	83.3 0.4	74.9 0.5	63.5 0.5	49.2 0.5	33.5 0.5	14.0 0.3
0.35	75.3 0.5	66.1 0.5	54.5 0.5	41.3 0.5	27.0 0.4	10.8 0.3
0.40	65.5 0.5	56.2 0.5	45.3 0.5	32.9 0.5	21.1 0.4	8.2 0.3
0.45	55.7 0.5	46.3 0.5	36.6 0.5	25.6 0.4	15.5 0.4	5.9 0.2
0.50	45.1 0.5	36.4 0.5	27.7 0.5	18.4 0.4	10.9 0.3	4.0 0.2
0.55	34.7 0.5	27.1 0.4	20.2 0.4	12.8 0.3	7.1 0.3	2.3 0.1
0.60	25.0 0.4	19.3 0.4	13.6 0.3	8.1 0.3	4.0 0.2	1.3 0.1
0.65	16.6 0.4	12.6 0.3	8.7 0.3	4.6 0.2	2.1 0.1	0.7 0.1
0.70	9.9 0.3	7.2 0.3	4.7 0.2	2.3 0.1	0.8 0.1	0.4 0.1
0.75	5.3 0.2	3.8 0.2	2.2 0.1	0.9 0.1	0.4 0.1	0.2 0.0
0.80	2.5 0.2	1.8 0.1	1.0 0.1	0.4 0.1	0.1 0.0	0.0 0.0
0.85	1.0 0.1	0.6 0.1	0.3 0.1	0.1 0.0	0.0 0.0	0.0 0.0
0.90	0.3 0.1	0.2 0.0	0.1 0.0	0.0 0.0	0.0 0.0	0.0 0.0
0.95	0.1 0.0	0.0 0.0	0.0 0.0	0.0 0.0	0.0 0.0	0.0 0.0
1.00	0.0 0.0	0.0 0.0	0.0 0.0	0.0 0.0	0.0 0.0	0.0 0.0

Table 4. (Continued)

(b) Percentage number transmission, 100 T_N; T_o= 6.0 MeV.

z/r_o	θ_o= 0°	30°	45°	60°	75°	89°
0.05	103.2±0.2	103.2±0.2	103.9±0.2	102.4±0.3	84.5±0.5	31.1±0.5
0.10	103.8 0.2	104.2 0.2	103.4 0.3	96.5 0.4	72.3 0.6	25.9 0.5
0.15	104.0 0.2	103.8 0.3	100.2 0.3	88.5 0.5	62.9 0.6	22.5 0.4
0.20	104.2 0.3	102.4 0.3	95.5 0.4	79.9 0.5	54.0 0.5	19.2 0.4
0.25	103.2 0.3	98.9 0.4	89.7 0.4	71.3 0.5	46.1 0.5	16.2 0.4
0.30	100.9 0.3	93.8 0.4	82.4 0.5	62.6 0.5	39.2 0.5	13.0 0.3
0.35	98.0 0.3	87.7 0.4	74.6 0.5	54.0 0.5	31.9 0.5	10.3 0.3
0.40	93.5 0.4	81.0 0.5	66.1 0.5	45.7 0.5	25.5 0.4	7.4 0.3
0.45	87.6 0.4	73.2 0.5	57.1 0.5	37.1 0.5	19.4 0.4	5.2 0.2
0.50	79.8 0.5	64.5 0.5	47.2 0.5	28.8 0.5	14.1 0.4	3.7 0.2
0.55	70.0 0.5	53.7 0.5	38.3 0.5	21.7 0.4	9.7 0.3	2.3 0.1
0.60	59.1 0.5	43.7 0.5	29.6 0.5	14.7 0.4	6.1 0.2	1.3 0.1
0.65	47.9 0.5	33.3 0.5	21.3 0.4	9.6 0.3	3.4 0.2	0.7 0.1
0.70	36.4 0.5	23.5 0.4	13.7 0.3	6.0 0.2	1.7 0.1	0.4 0.1
0.75	25.3 0.4	15.3 0.4	8.2 0.3	3.1 0.2	0.7 0.1	0.2 0.0
0.80	15.5 0.4	8.5 0.3	4.4 0.2	1.5 0.1	0.2 0.0	0.1 0.0
0.85	8.4 0.3	4.2 0.2	1.8 0.1	0.8 0.1	0.1 0.0	0.0 0.0
0.90	3.9 0.2	1.9 0.1	0.7 0.1	0.2 0.0	0.1 0.0	0.0 0.0
0.95	1.4 0.1	0.6 0.1	0.2 0.0	0.1 0.0	0.1 0.0	0.1 0.0
1.00	0.4 0.1	0.2 0.0	0.2 0.0	0.1 0.0	0.0 0.0	0.0 0.0

Table 4. (Continued)

(c) Percentage energy transmission, 100 T_E; T_o = 1.0 MeV.

z/r_o	θ_o= 0°	30°	45°	60°	75°	89°
0.05	96.0	94.9	91.9	81.0	57.5	23.7
0.10	90.8	87.1	79.2	64.3	44.3	18.2
0.15	83.8	77.1	67.1	52.3	34.9	14.3
0.20	75.2	66.7	56.2	42.4	27.9	11.4
0.25	65.6	56.7	46.1	34.3	22.0	8.8
0.30	55.5	47.0	37.4	26.9	16.9	6.7
0.35	45.7	37.8	29.3	20.6	12.4	4.7
0.40	36.1	29.3	22.3	15.0	8.8	3.3
0.45	27.7	21.9	16.3	10.5	6.0	2.1
0.50	20.3	15.6	11.2	6.9	3.8	1.3
0.55	13.9	10.5	7.4	4.3	2.2	0.7
0.60	8.9	6.6	4.4	2.5	1.1	0.4
0.65	5.3	3.8	2.5	1.2	0.5	0.2
0.70	2.8	2.0	1.2	0.5	0.2	0.1
0.75	1.4	0.9	0.5	0.2	0.1	0.0
0.80	0.6	0.4	0.2	0.1	0.0	0.0
0.85	0.2	0.1	0.0	0.0	0.0	0.0
0.90	0.1	0.0	0.0	0.0	0.0	0.0
0.95	0.0	0.0	0.0	0.0	0.0	0.0
1.00	0.0	0.0	0.0	0.0	0.0	0.0

Table 4. (Continued)

(d) Percentage energy transmission, 100 T_E; T_o = 6.0 MeV.

z/r_o	θ_o= 0°	30°	45°	60°	75°	89°
0.05	95.2	94.3	92.7	86.3	62.4	20.8
0.10	90.1	88.1	83.3	69.8	45.0	14.6
0.15	84.6	80.8	72.6	56.4	34.0	10.9
0.20	78.6	72.6	62.0	44.9	25.9	8.2
0.25	72.2	63.7	52.1	35.8	19.7	6.2
0.30	64.9	54.9	43.1	28.1	15.0	4.4
0.35	57.3	46.5	34.9	21.8	11.0	3.1
0.40	49.3	38.6	27.8	16.6	7.9	2.0
0.45	41.1	31.0	21.5	12.0	5.4	1.3
0.50	33.3	24.2	16.0	8.4	3.5	0.8
0.55	25.9	18.0	11.5	5.6	2.1	0.5
0.60	19.2	12.9	7.8	3.4	1.2	0.3
0.65	13.6	8.6	4.9	2.0	0.6	0.1
0.70	9.0	5.3	2.8	1.1	0.2	0.1
0.75	5.3	2.9	1.4	0.5	0.1	0.0
0.80	2.8	1.4	0.6	0.2	0.0	0.0
0.85	1.3	0.6	0.2	0.1	0.0	0.0
0.90	0.5	0.2	0.1	0.0	0.0	0.0
0.95	0.2	0.1	0.0	0.0	0.0	0.0
1.00	0.0	0.0	0.0	0.0	0.0	0.0

Table 5. Transmission of electrons by plane-parallel aluminum targets. Electrons are assumed to be incident on a target of thickness z with a cosine-law distribution of angles of incidence, and with various kinetic energies between 0.5 MeV and 10.0 MeV.

(a) Percentage number transmission, 100 T_N.

z/r_o	T_o= 0.5	1.0	2.0	4.0	6.0	8.0	10.0 MeV
0.05	92.5±0.3	93.1±0.3	94.5±0.3	97.9±0.3	99.6±0.3	100.9±0.3	101.3±0.3
0.10	85.3 0.4	87.4 0.4	88.5 0.4	94.0 0.4	97.1 0.4	98.1 0.4	99.0 0.4
0.15	78.7 0.4	81.7 0.4	82.6 0.4	89.4 0.4	93.3 0.4	94.6 0.4	95.6 0.4
0.20	72.1 0.5	75.7 0.5	76.5 0.5	84.1 0.5	88.3 0.5	89.9 0.4	91.4 0.5
0.25	64.6 0.5	68.3 0.5	69.7 0.5	78.6 0.5	82.6 0.5	84.5 0.5	85.7 0.5
0.30	56.7 0.5	60.7 0.5	62.5 0.5	71.6 0.5	75.9 0.5	79.4 0.5	80.4 0.5
0.35	48.8 0.5	52.7 0.5	55.1 0.5	64.9 0.5	69.5 0.5	71.7 0.5	73.8 0.5
0.40	40.9 0.5	45.4 0.5	47.0 0.5	57.4 0.5	62.3 0.5	65.0 0.5	67.0 0.5
0.45	32.7 0.5	37.2 0.5	39.0 0.5	48.9 0.5	54.9 0.5	57.2 0.5	59.5 0.5
0.50	25.2 0.4	29.4 0.5	30.8 0.5	40.7 0.5	46.4 0.5	49.3 0.5	52.0 0.5
0.55	18.4 0.4	21.9 0.4	23.2 0.4	32.6 0.5	38.0 0.5	41.4 0.5	43.6 0.5
0.60	12.2 0.3	15.3 0.4	16.6 0.4	24.5 0.4	30.1 0.5	33.2 0.5	36.5 0.5
0.65	7.6 0.3	9.8 0.3	11.4 0.3	17.4 0.4	22.5 0.4	25.1 0.4	28.1 0.5
0.70	4.5 0.2	5.9 0.2	6.8 0.3	11.5 0.3	15.2 0.4	17.6 0.4	21.2 0.4
0.75	2.3 0.1	3.1 0.2	3.6 0.2	6.9 0.3	9.6 0.3	11.7 0.3	14.6 0.4
0.80	0.9 0.1	1.5 0.1	1.7 0.1	3.5 0.2	5.3 0.2	6.6 0.2	8.9 0.3
0.85	0.3 0.1	0.5 0.1	0.7 0.1	1.4 0.1	2.7 0.2	3.5 0.2	5.0 0.2
0.90	0.1 0.0	0.2 0.0	0.2 0.0	0.5 0.1	1.1 0.1	1.8 0.1	2.5 0.2
0.95	0.0 0.0	0.1 0.0	0.0 0.0	0.1 0.0	0.4 0.1	0.6 0.1	1.1 0.1
1.00	0.0 0.0	0.0 0.0	0.0 0.0	0.1 0.0	0.3 0.1	0.3 0.1	0.7 0.1

Table 5. (Continued)

(b) Percentage energy transmission, 100 T_E.

z/r_o	T_o= 0.5	1.0	2.0	4.0	6.0	8.0	10.0 MeV
0.05	85.5	85.1	85.1	86.4	87.0	87.2	87.4
0.10	73.3	73.8	72.9	75.6	76.4	76.6	76.7
0.15	62.7	63.4	62.4	65.3	66.6	66.8	67.1
0.20	53.1	54.1	52.9	56.0	57.4	57.8	58.2
0.25	44.1	44.8	44.0	47.5	48.9	49.6	49.8
0.30	35.7	36.7	36.1	39.5	41.1	42.1	42.4
0.35	28.4	29.4	28.9	32.4	34.1	34.9	35.4
0.40	21.7	23.0	22.3	25.9	27.7	28.5	29.1
0.45	16.0	17.0	16.6	19.9	21.8	22.7	23.4
0.50	11.1	12.3	11.8	14.9	16.6	17.6	18.2
0.55	7.4	8.3	8.0	10.6	12.2	13.2	13.8
0.60	4.4	5.2	5.1	7.0	8.4	9.3	10.1
0.65	2.5	3.0	3.1	4.4	5.6	6.2	7.0
0.70	1.3	1.6	1.6	2.6	3.3	3.8	4.6
0.75	0.6	0.8	0.8	1.3	1.8	2.2	2.7
0.80	0.2	0.3	0.3	0.6	0.9	1.1	1.5
0.85	0.1	0.1	0.1	0.2	0.4	0.5	0.7
0.90	0.0	0.0	0.0	0.1	0.1	0.2	0.3
0.95	0.0	0.0	0.0	0.0	0.1	0.1	0.1
1.00	0.0	0.0	0.0	0.0	0.0	0.0	0.1

Figures

Fig. 1. Number reflection coefficient R_N for electrons incident perpendicularly on aluminum targets of saturation thickness. The calculated coefficient as a function of the incident electron energy is compared with the experimental values of Miller and Hendricks[15], Ebert et al.[16], Agu et al.[17], Nakai et al.[18], Tabata[19], Cohen and Koral[20], Saldick and Allen[21], Jakschik and Jüngst[22], Miller[23], Rester et al.[24], Wright and Trump[25], Frank[26], Dressel[27], Harder and Ferbert[28], Glazunov and Guglya[29], and Trump and Van de Graaff[30].

Fig. 2. Number reflection coefficient R_N for aluminum as a function of the angle of incidence, θ_o. Target has saturation thickness. The calculated curve is compared with the experimental results of Cohen and Koral[20], Miller and Hendricks[15], Okabe et al.[31], and Tabata[19].

Fig. 3. Energy reflection coefficient R_E for electrons incident perpendicularly on aluminum targets of saturation thickness. The calculated curve of R_E *vs* the incident electron energy T_o is compared with the experimental results of Rester et al.[24] and Wright and Trump[25].

Fig. 4. Number transmission coefficient T_N for electrons incident perpendicularly, with kinetic energy T_o, on plane-parallel aluminum targets of thickness z. The solid curves are calculated values of T_N and pertain to the transmitted charge. The dashed curves are calculated such that the emergence of a primary electron and one or more associated secondary electrons is treated as a single "transmission event", which

Fig. 4. (continued)

corresponds to the experimental conditions of Seliger[32] and Harder and Poschet[33].

a. T_0 = 0.25 MeV; comparison with results of Seliger[32] and Miller and Hendricks[15];

b. T_0 = 0.5 MeV; comparison with results of Agu et al.[17] and Miller and Hendricks[15];

c. T_0 = 0.75 MeV; comparison with experimental results of Agu et al.[17] at 0.7 MeV, Nakai et al.[18] at 0.8 MeV, and Miller and Hendricks[15] at 0.75 MeV;

d. T_0 = 1.0 MeV; comparison with the results of Seliger[32] at 0.96 MeV, and of Nakai et al.[18], Miller and Hendricks[15], and Miller[23] at 1.0 MeV;

e. T_0 = 2.0 MeV; comparison with experimental results of Miller[23];

f. T_0 = 3.0 MeV; comparison with experimental results of Miller[23];

g. T_0 = 4.0 MeV; comparison with experimental results of Ebert et al.[16] at 4.0 MeV, and Harder and Poschet[33] at 4.17 MeV;

h. T_0 = 10.0 MeV; comparison with experimental results of Ebert et al.[16] at 10.0 MeV, and Harder and Poschet[33] at 10.83 MeV.

Fig. 5. Number transmission coefficient T_N for electrons incident on a plane-parallel aluminum target of thickness z with energy T_0 and with obliquity angle $\theta_0 = 45^\circ$. As in Fig. 4, solid curves pertain to transmitted charge, and dashed curves to "transmission events". Comparisons are made with experimental results of Miller and Hendricks[15] who measured transmitted charge.

a. T_0 = 0.25 MeV;

b. T_0 = 0.5 MeV;

c. T_0 = 0.75 MeV;

d. T_0 = 1.0 MeV.

Fig. 6. Number transmission coefficient T_N for 10-MeV electrons incident perpendicularly on plane-parallel Be, C, Al, Cu, Ag, and Pb targets.

The results for Be are entirely theoretical (curve 1: includes primary and secondary electrons, based on complete treatment of energy-loss straggling; curve 2: (dashed) - includes primary electrons only, based on complete treatment of energy-loss straggling; curve 3: includes primary electrons only, energy loss treated in continuous-slowing-down-approximation). For the other media, the calculated curves correspond to curve 1 for Be.

Comparisons are made with experimental results of Ebert et al.[16] [open points (o)] and Harder[34] [solid points (●)]. The experimental points accompanying the calculated curve for Pb (Z=82) are actually results obtained by Ebert et al.[16] for Ta (Z=73) [open points (o)] and for U (Z=92) [open squares (□)].

Fig. 7. Bremsstrahlung efficiency Y for 6.0-MeV electrons incident at various angles on a plane-parallel aluminum target of thickness z.

Fig. 8. Distribution with respect to depth of the charge deposited by electrons incident perpendicularly on plane-parallel targets. The distribution $D_c(z)$ represents the amount of charge, per incident electron, that is deposited at depth z per unit layer of the target. Actually plotted is the dimensionless quantity $r_o D_c(z)/e$, where r_o is the c.s.d.a. range of the incident electrons and e is the electronic charge. A negative value of $D_c(z)$ indicates charge depletion due to the escape of secondary electrons.

Fig. 8. (continued)

a. Semi-infinite Al medium; T_o = 3 MeV; experimental points (o) from Gross and Wright[35];
b. Semi-infinite Al medium; T_o = 4 MeV; curve from experiment of Tabata et al.[36] at 4.05 MeV;
c. Semi-infinite Be medium; T_o = 10 MeV; points (o) from experiment of Tabata et al.[36] at 11.5 MeV. Dotted histogram is from a calculation using the continuous-slowing-down-approximation.
d. Semi-infinite Al medium; T_o = 10 MeV; points (o) from experiment of Tabata et al.[36] at 11.5 MeV;
e. Cu slab with thickness 0.8 r_o; T_o = 10 MeV; points (o) from experiment of Tabata et al.[36] at 11.5 MeV in semi-infinite medium;
f. Ag slab with thickness 0.8 r_o; T_o = 10 MeV; points (o) from experiment of Tabata et al.[36] at 11.5 MeV in semi-infinite medium;
g. Pb slab with thickness 0.6 r_o; T_o = 10 MeV; points (o) from experiment of Tabata et al.[36] at 11.5 MeV in semi-infinite Au medium.

Fig. 9. Ratio of practical range r_p to incident electron kinetic energy T_o, for plane-parallel aluminum targets. The Monte Carlo curve of r_p/T_o vs T_o is compared with the empirical formula of Katz and Penfold[38] and with experimental results of Seliger[32], Miller and Hendricks[15], Harder and Poschet[33], Agu et al.[17], Horikiri et al.[39], Ebert et al.[16], and Miller[23].

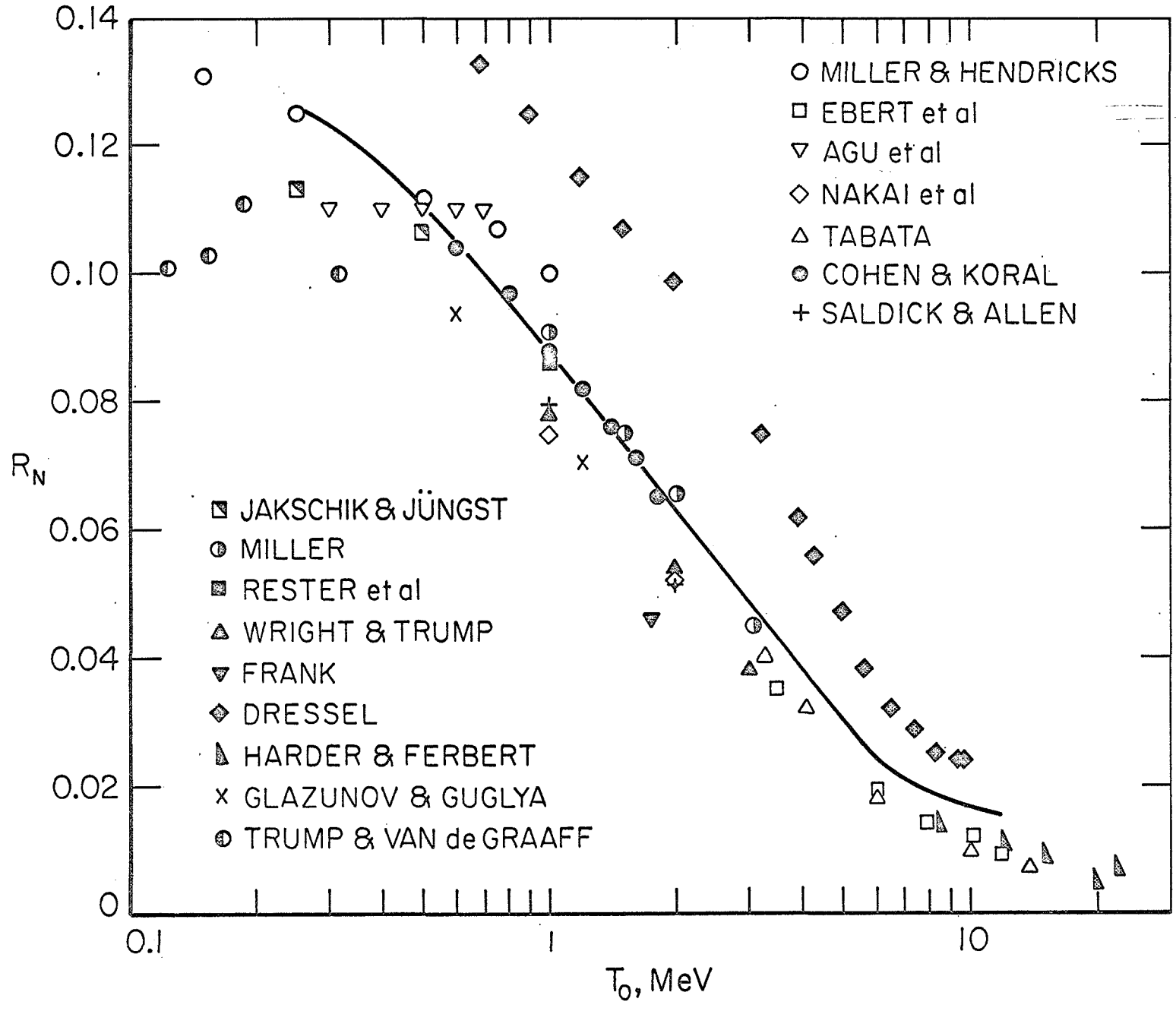
0.14
0.12
0.10
0.08
0.06
0.04
0.02
0
R_N
0.1
1
10
T_0, MeV
MILLER & HENDRICKS
EBERT et al
AGU et al
NAKAI et al
TABATA
COHEN & KORAL
SALDICK & ALLEN
JAKSCHIK & JÜNGST
MILLER
RESTER et al
WRIGHT & TRUMP
FRANK
DRESSEL
HARDER & FERBERT
GLAZUNOV & GUGLYA
TRUMP & VAN de GRAAFF

Fig. 1

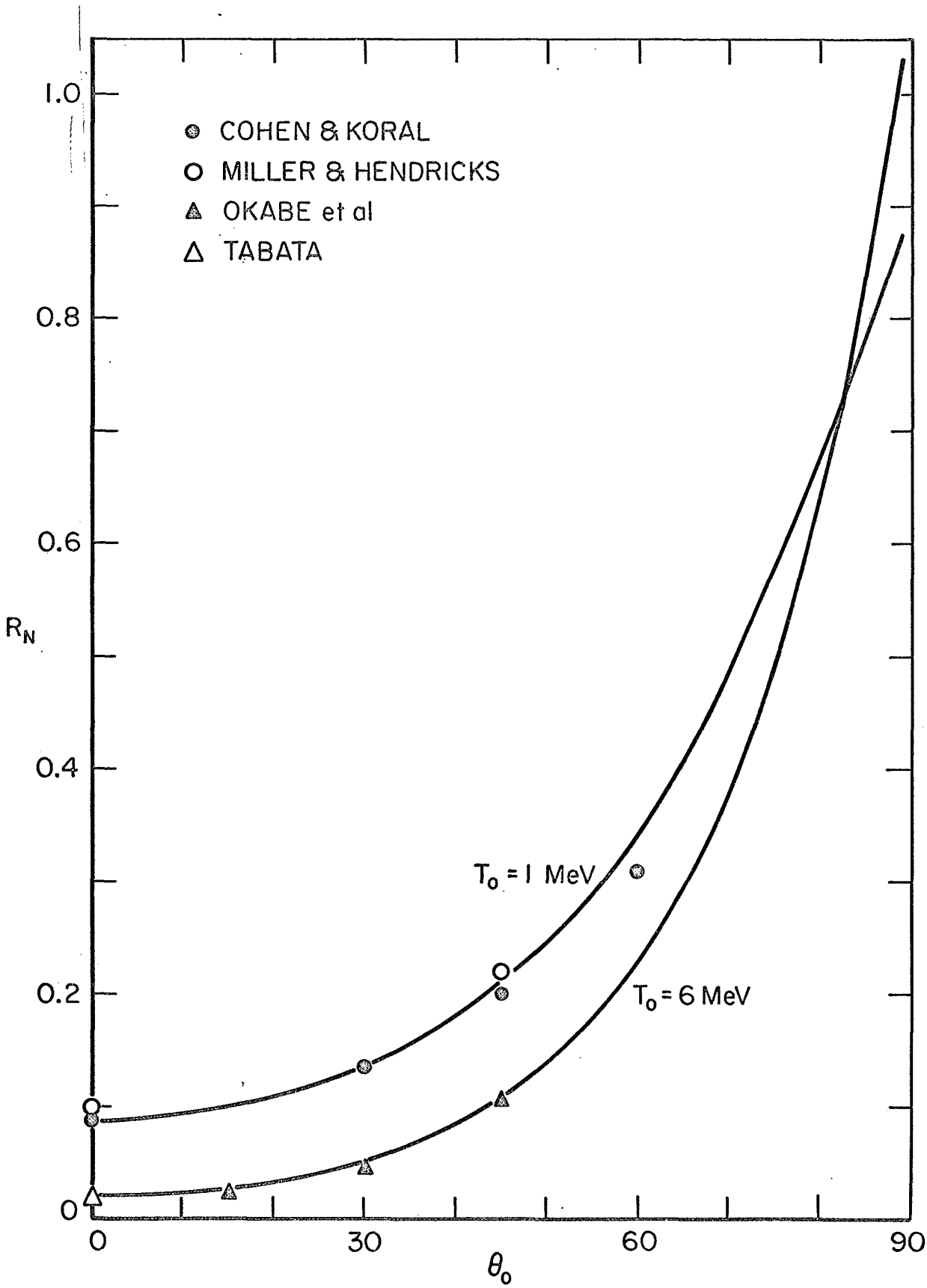
1.0
0.8
0.6
0.4
0.2
0
R_N
COHEN & KORAL
MILLER & HENDRICKS
OKABE et al
TABATA
T_0 = 1 MeV
T_0 = 6 MeV
0
30
60
90
θ_0

Fig. 2

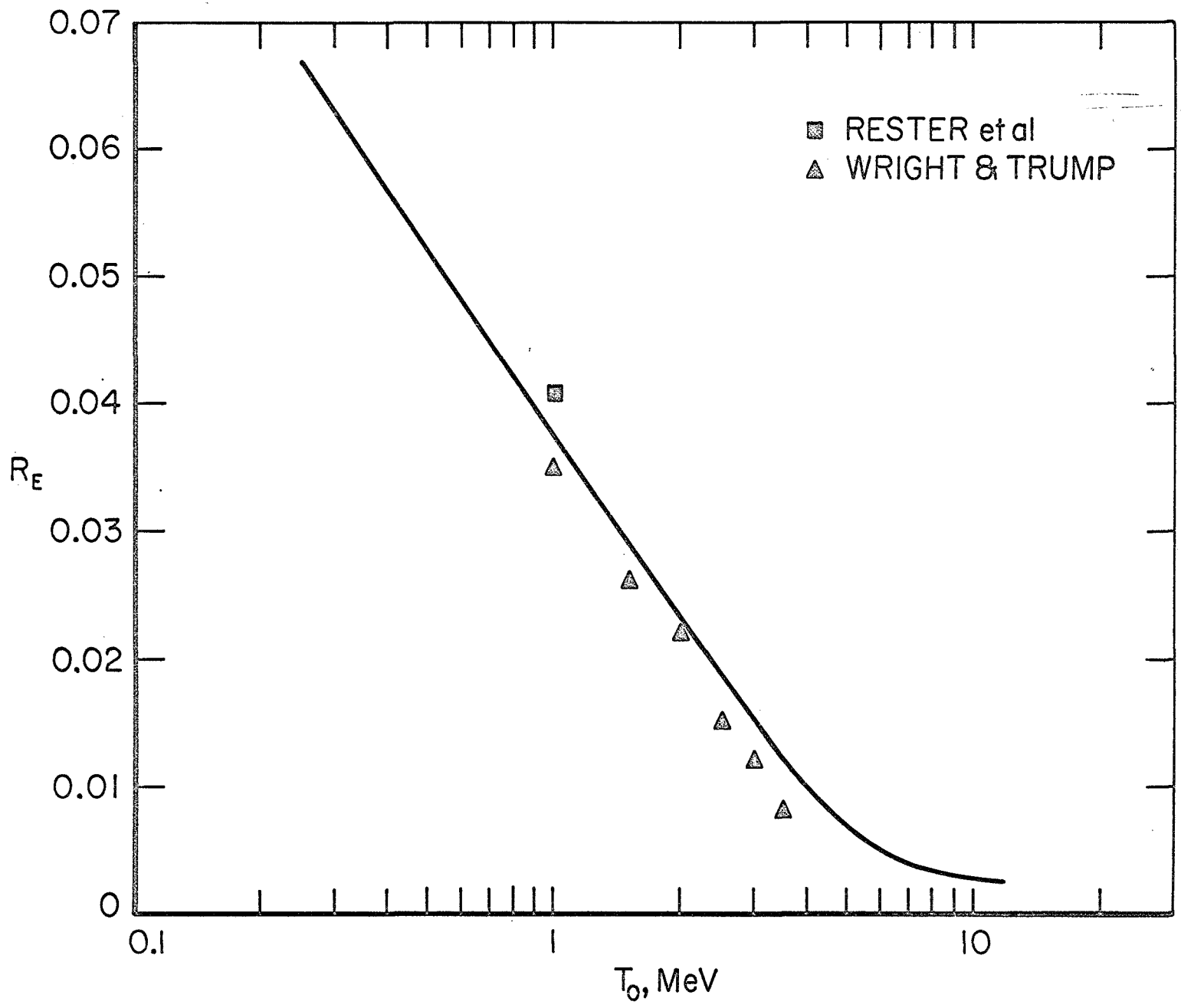
0.07
0.06
0.05
0.04
0.03
0.02
0.01
0
R_E
0.1
1
10
T_o, MeV
RESTER et al
WRIGHT & TRUMP

Fig. 3

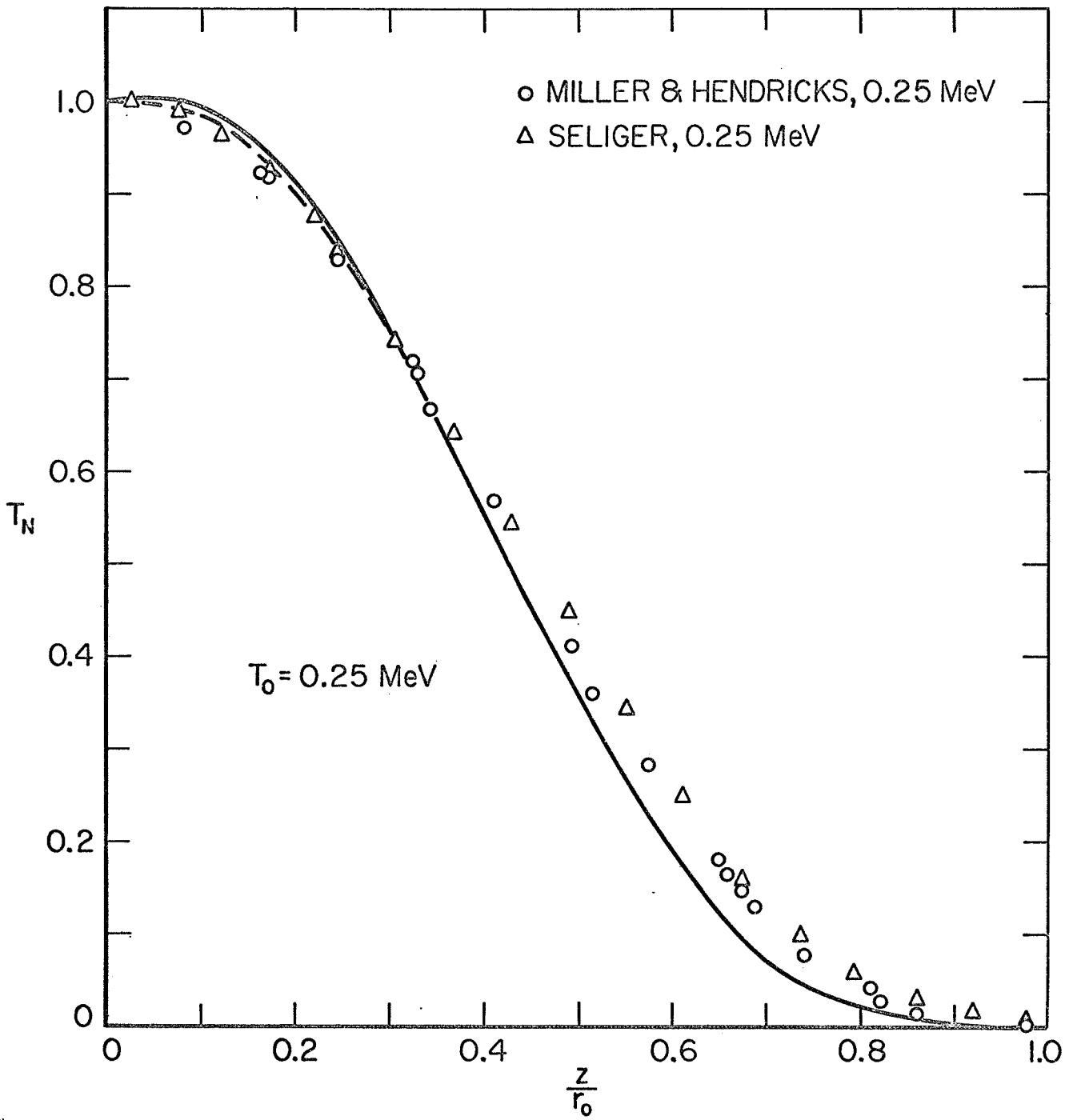
o MILLER & HENDRICKS, 0.25 MeV
Δ SELIGER, 0.25 MeV
T_N
T_0 = 0.25 MeV
1.0
0.8
0.6
0.4
0.2
0
0
0.2
0.4
0.6
0.8
1.0
$\frac{z}{r_0}$

Fig. 4a

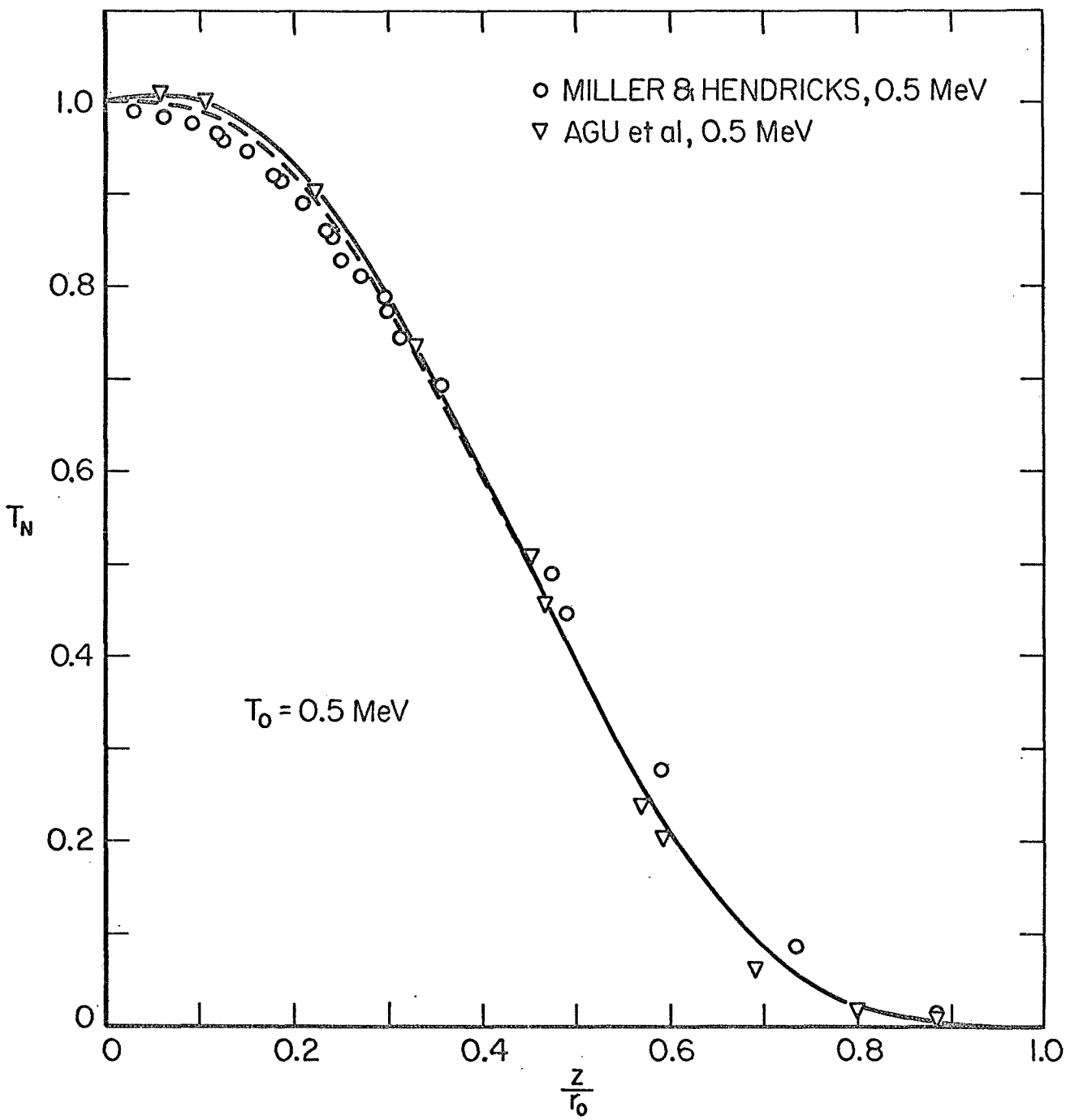
MILLER & HENDRICKS, 0.5 MeV
AGU et al, 0.5 MeV
T_0 = 0.5 MeV
T_N
$\frac{z}{r_0}$
0
0.2
0.4
0.6
0.8
1.0

Fig. 4b

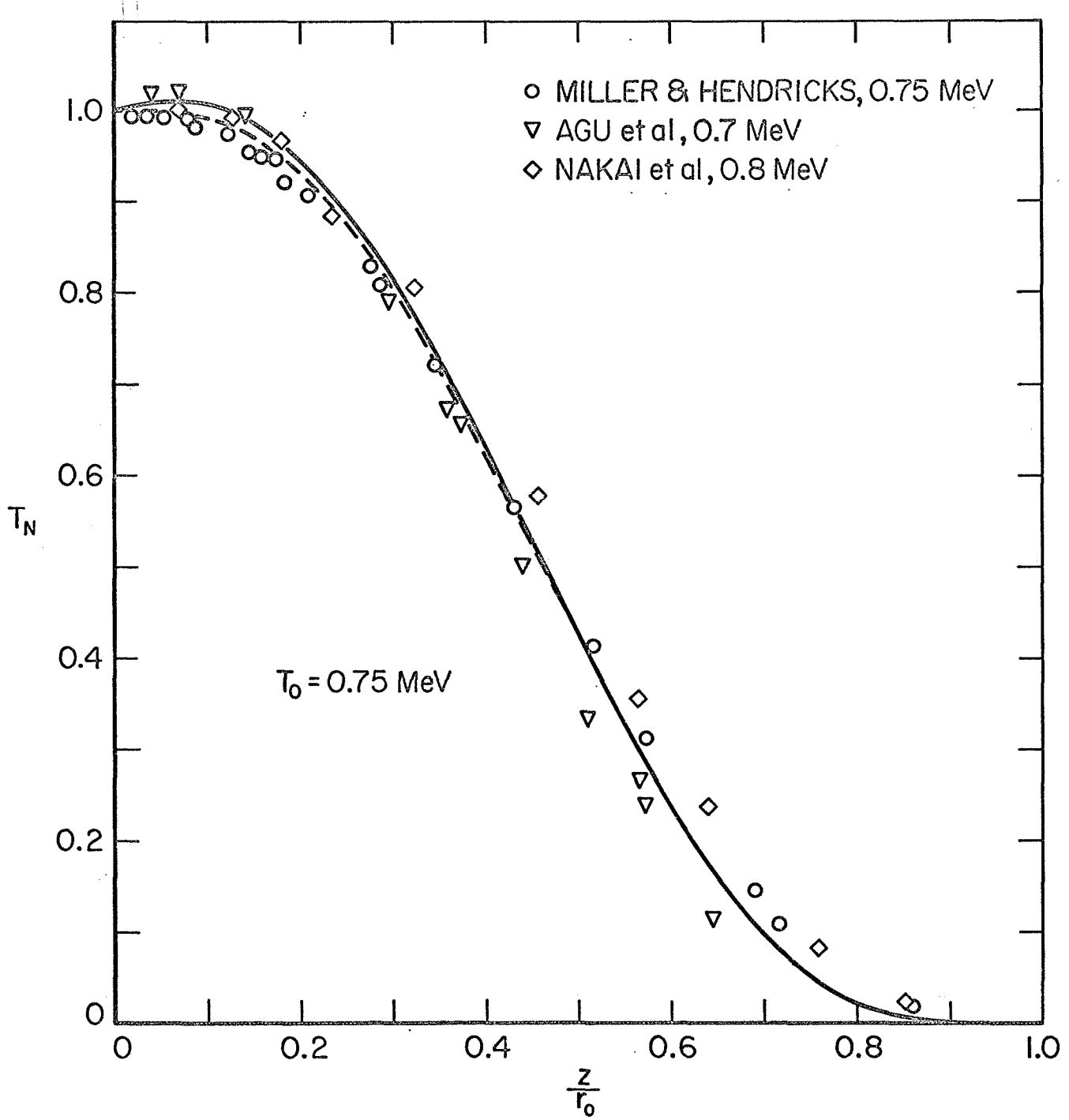
MILLER & HENDRICKS, 0.75 MeV
AGU et al, 0.7 MeV
NAKAI et al, 0.8 MeV
T_0 = 0.75 MeV
T_N
$\frac{z}{r_0}$
0
0.2
0.4
0.6
0.8
1.0

Fig. 4c

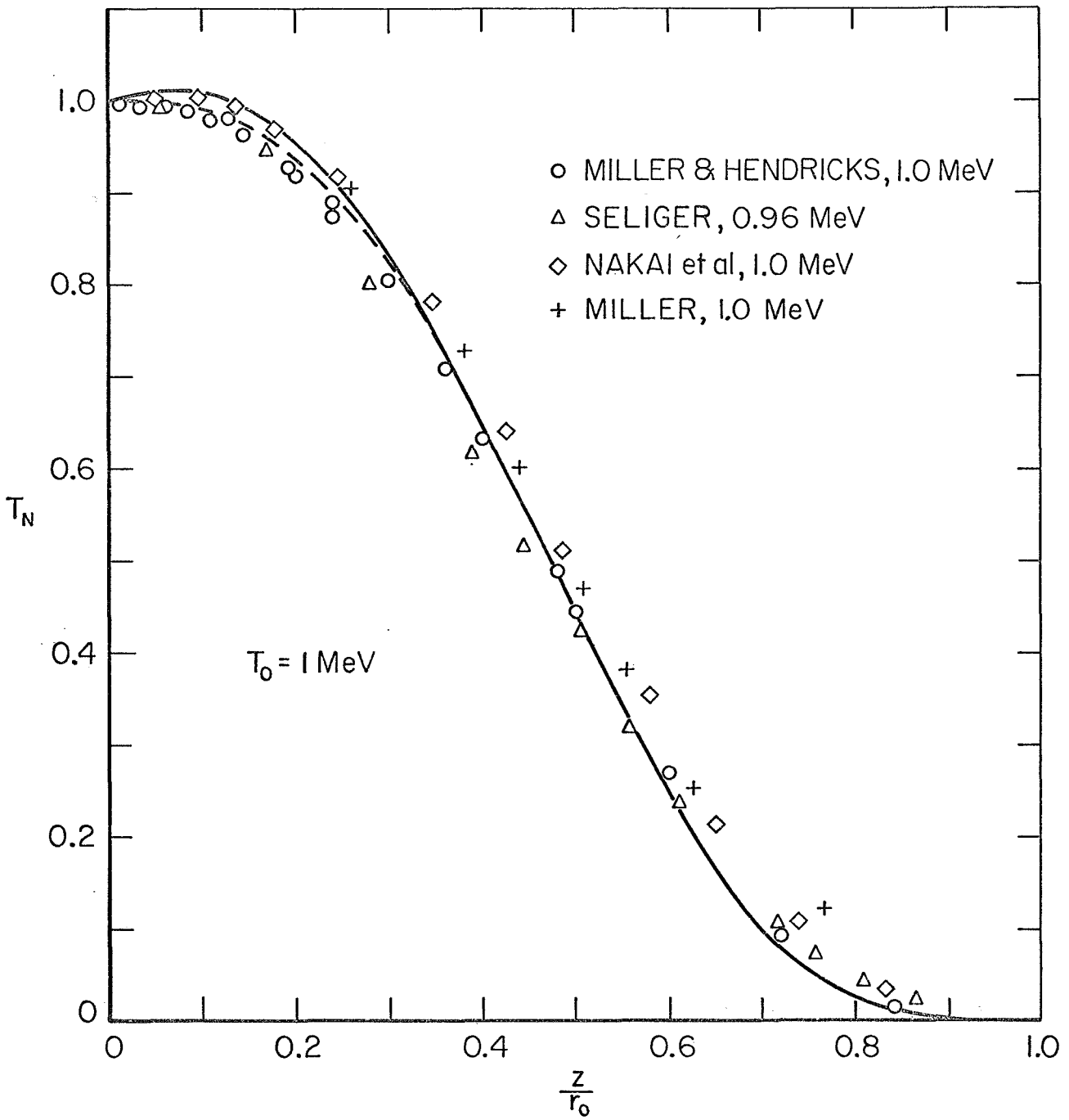
1.0
0.8
0.6
0.4
0.2
0
T_N
0
0.2
0.4
0.6
0.8
1.0
$\frac{z}{r_0}$
MILLER & HENDRICKS, 1.0 MeV
SELIGER, 0.96 MeV
NAKAI et al, 1.0 MeV
MILLER, 1.0 MeV
T_0 = 1 MeV

Fig. 4d

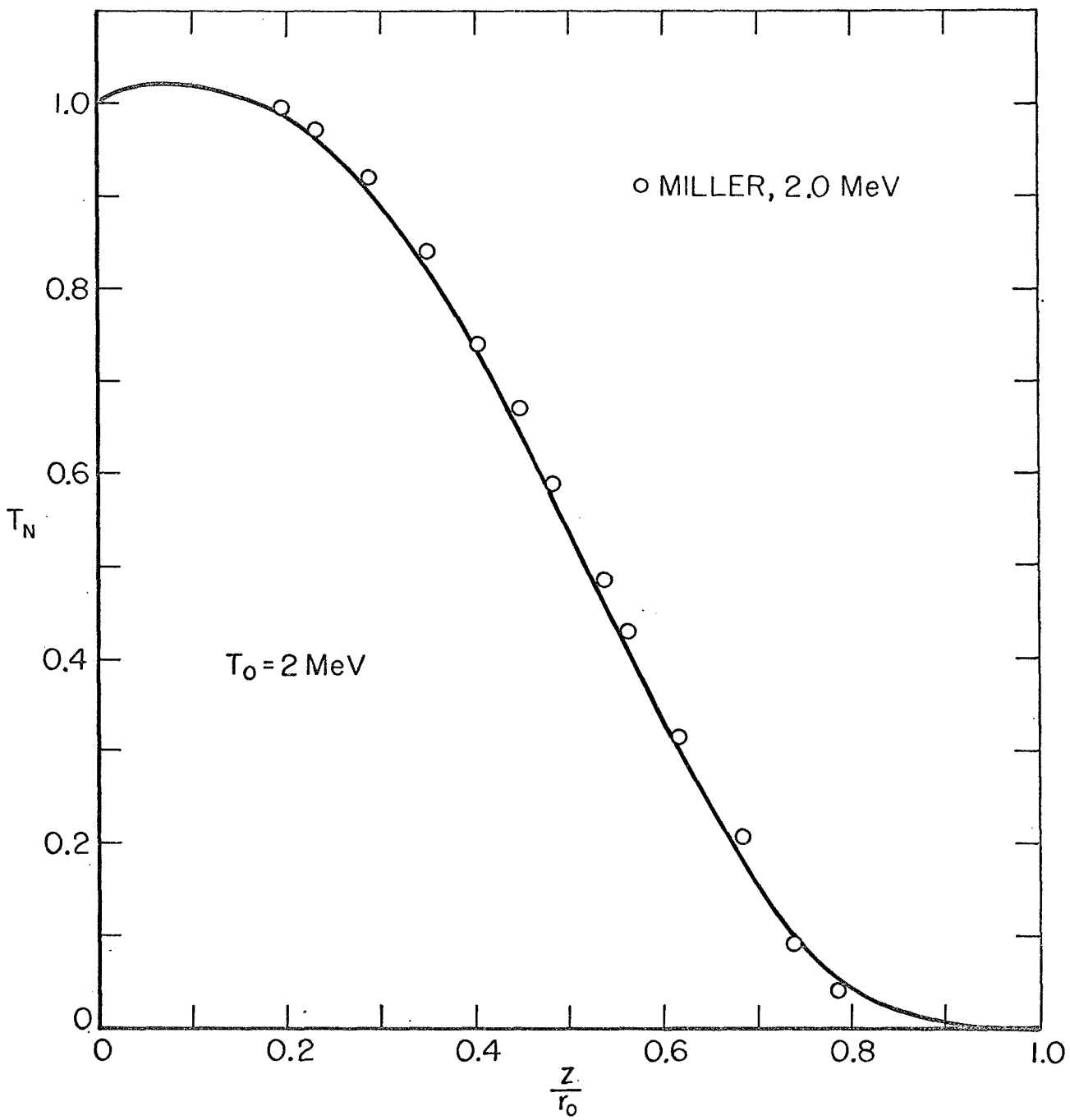

Fig. 4e

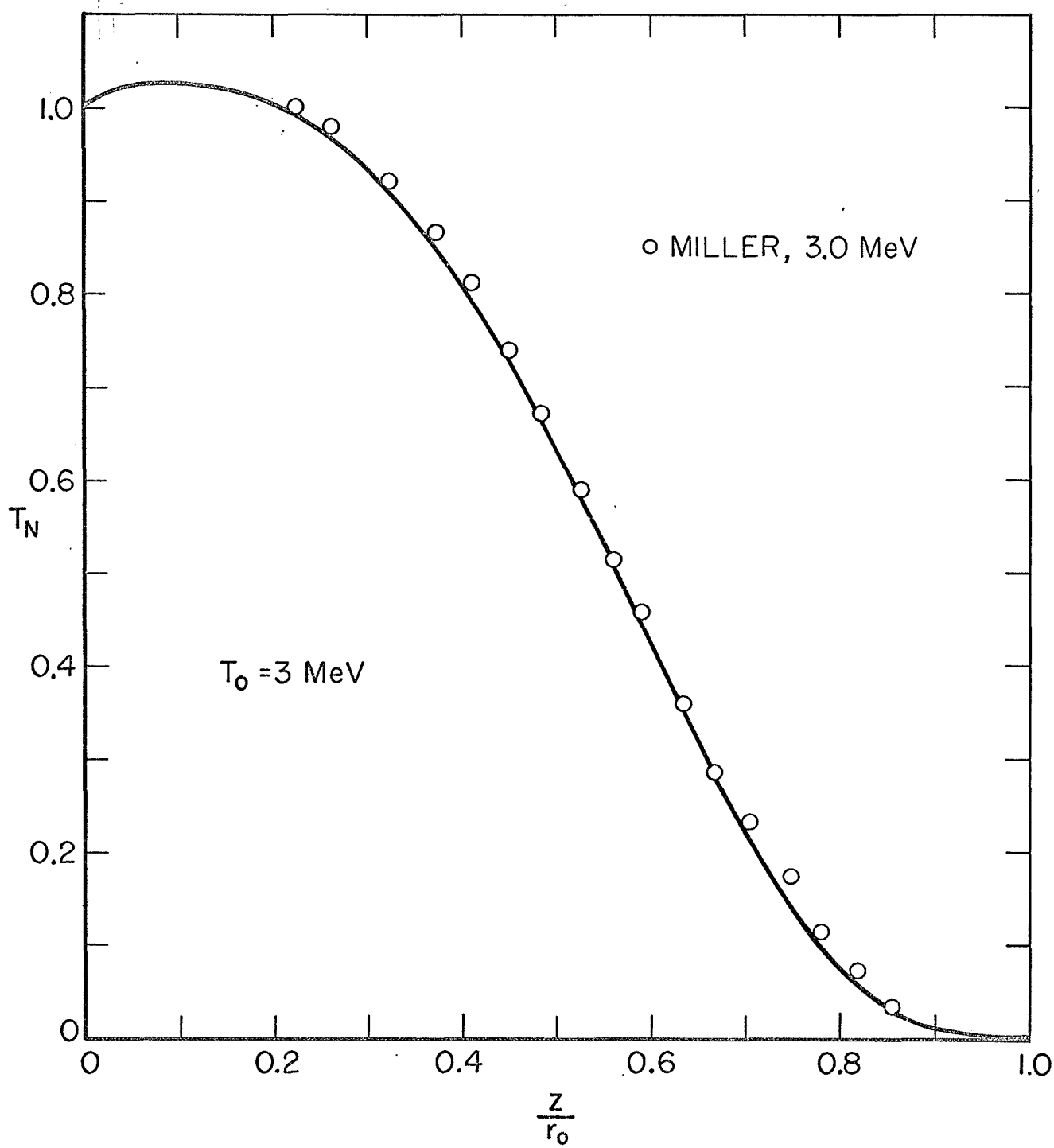

Fig. 4f

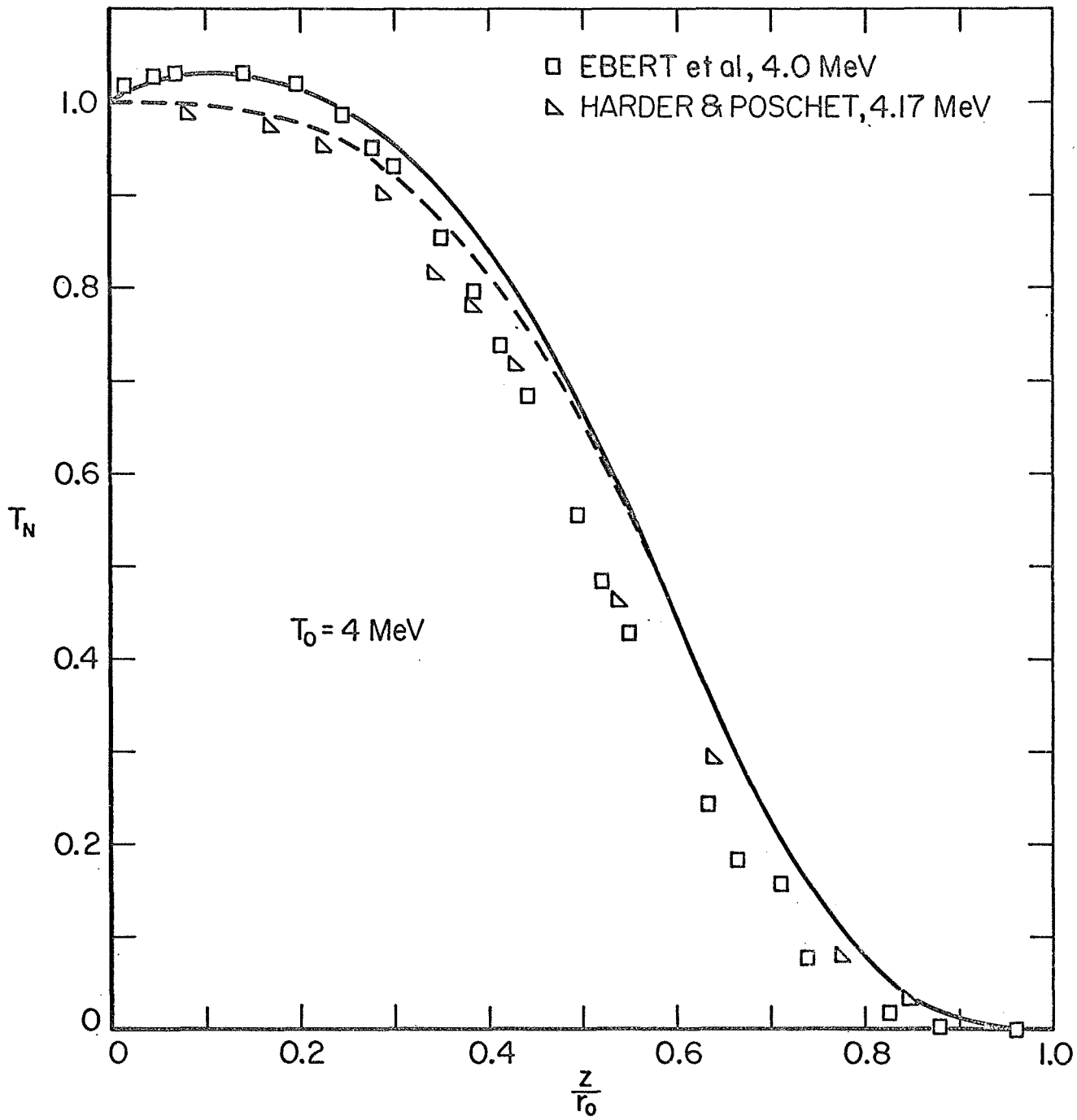
EBERT et al, 4.0 MeV
HARDER & POSCHET, 4.17 MeV
T_0 = 4 MeV
T_N
$\frac{z}{r_0}$
0
0.2
0.4
0.6
0.8
1.0

Fig. 4g

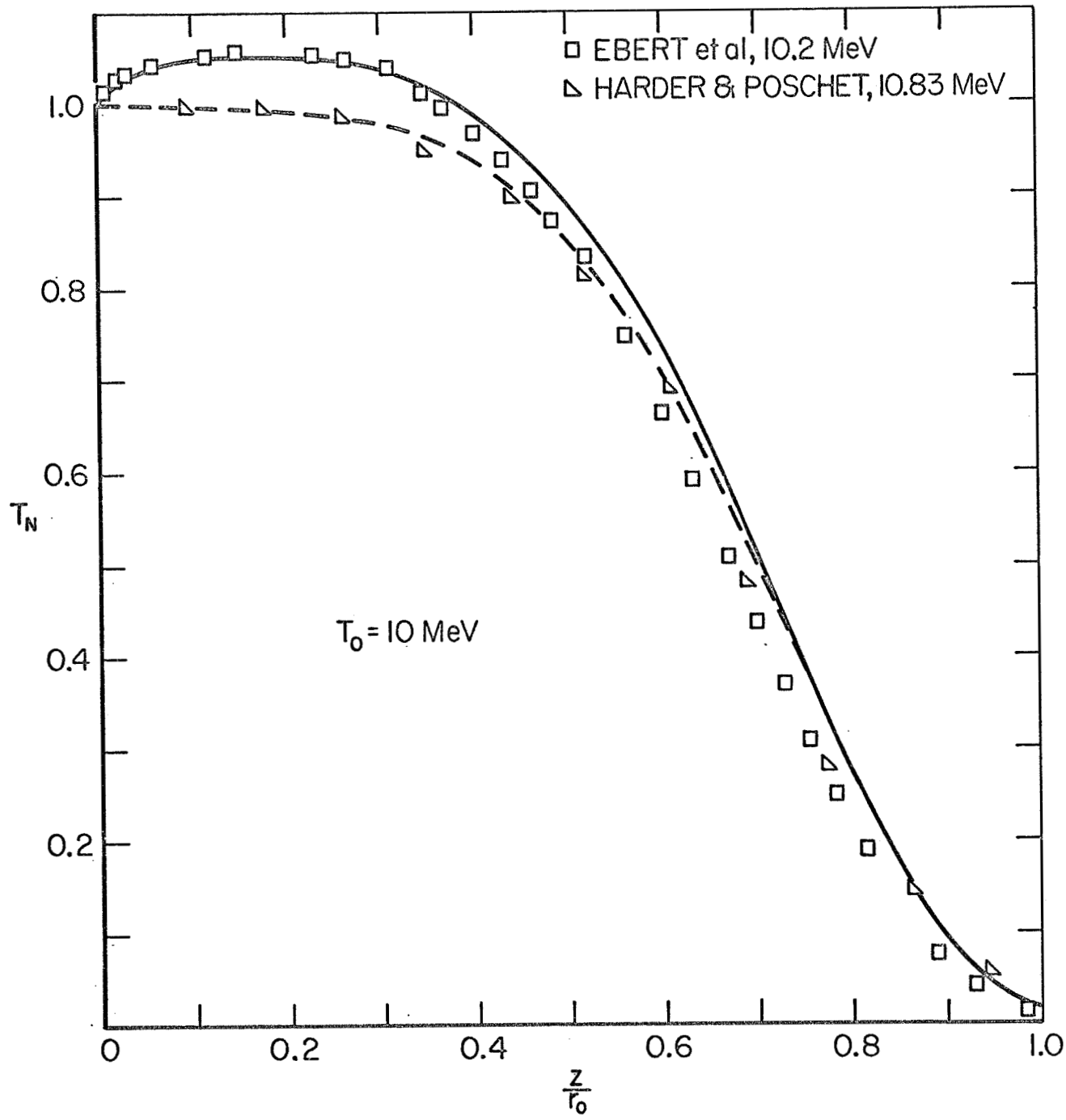
EBERT et al, 10.2 MeV
HARDER & POSCHET, 10.83 MeV
T_0 = 10 MeV
T_N
1.0
0.8
0.6
0.4
0.2
0
0.2
0.4
0.6
0.8
1.0
$\frac{z}{r_0}$

Fig. 4h

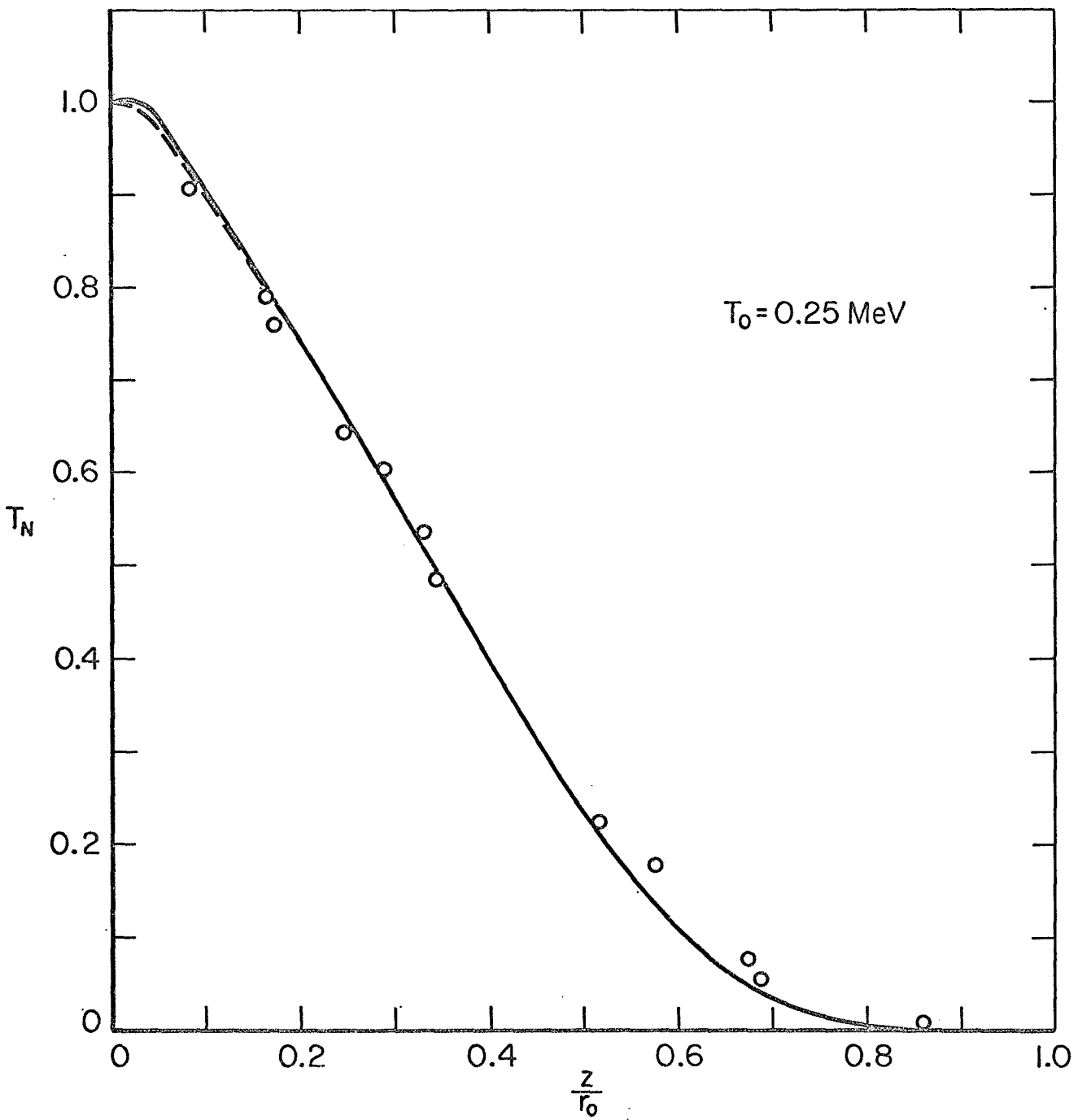

Fig. 5a

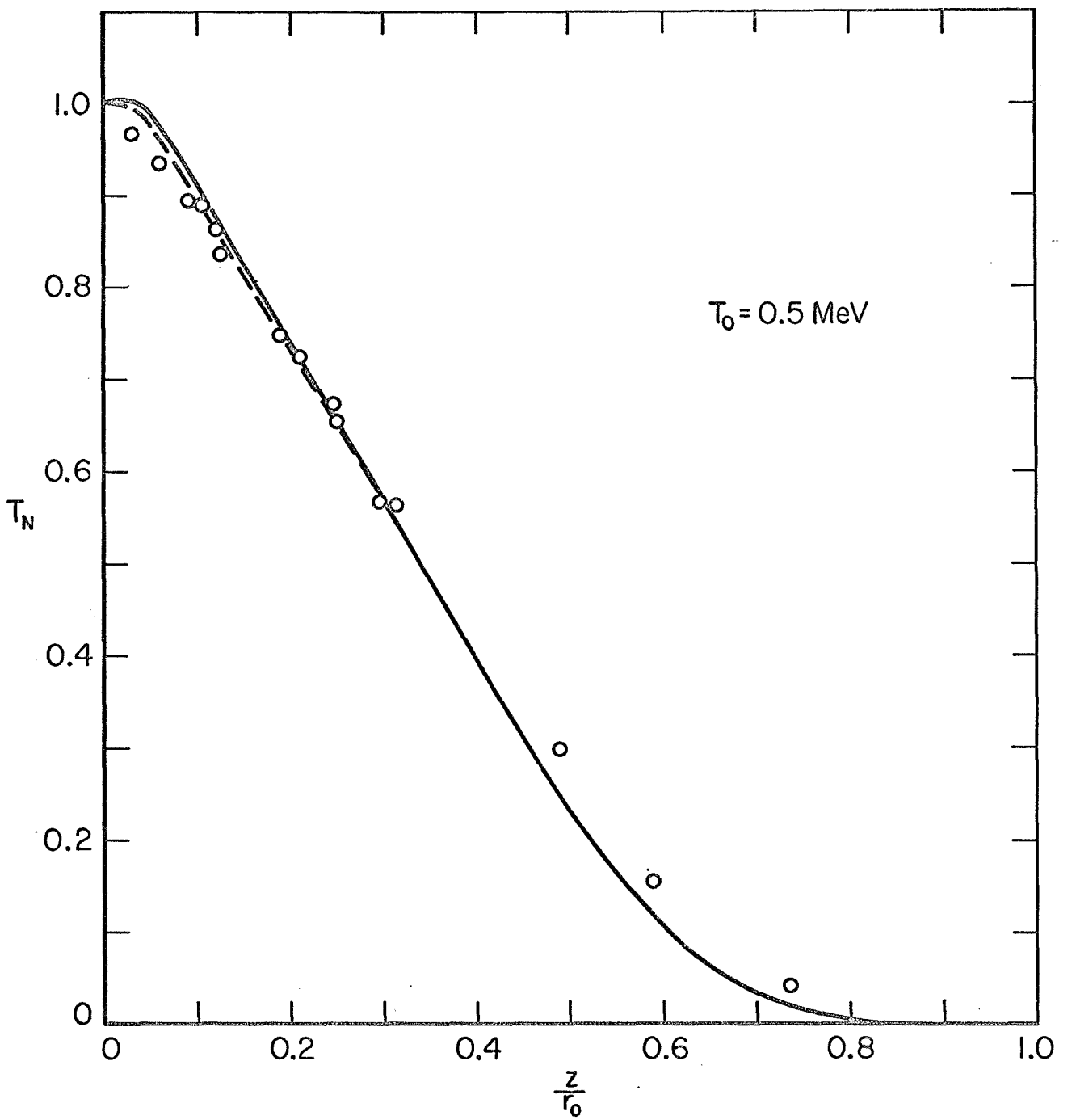

Fig. 5b

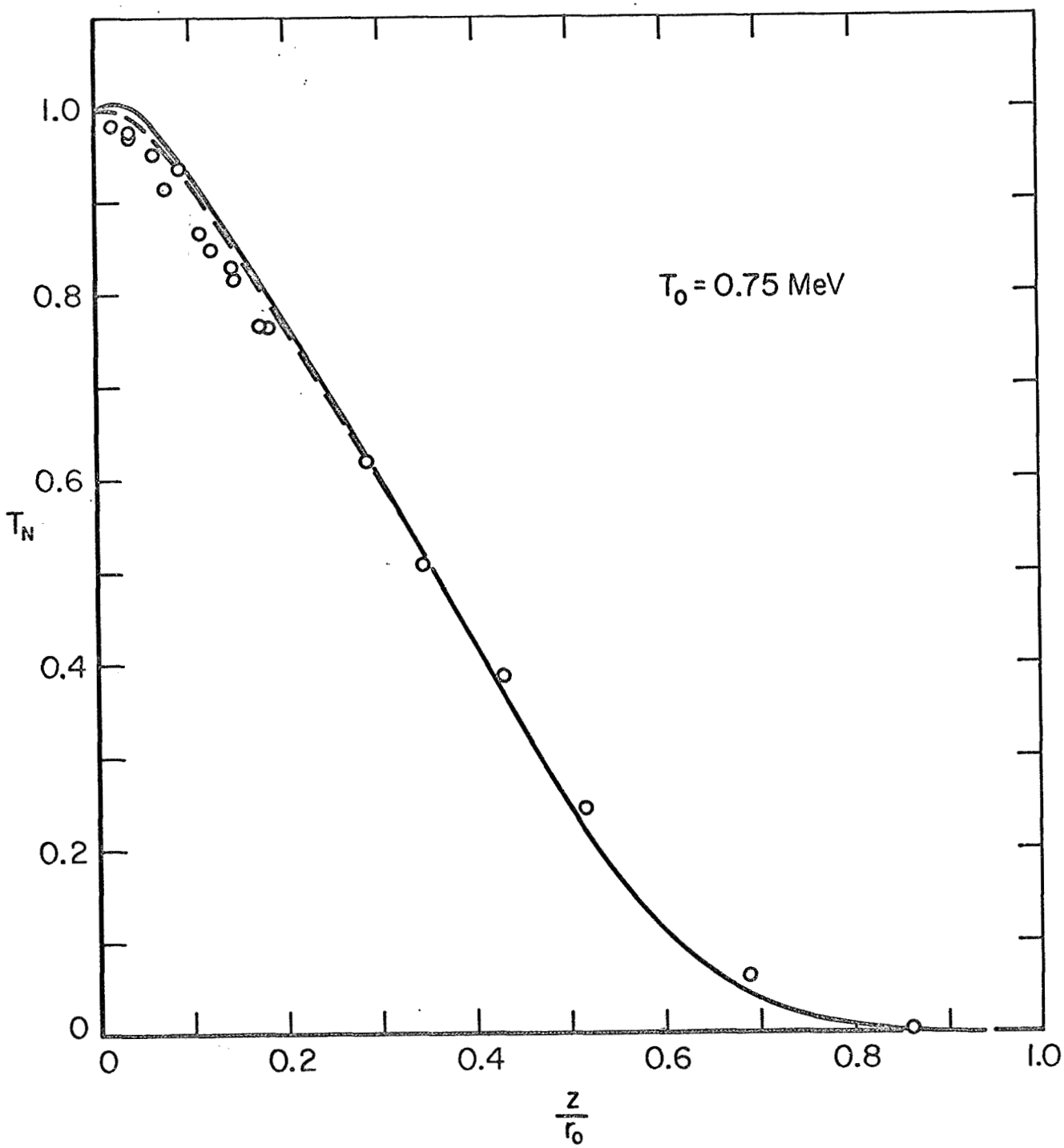

Fig. 5c

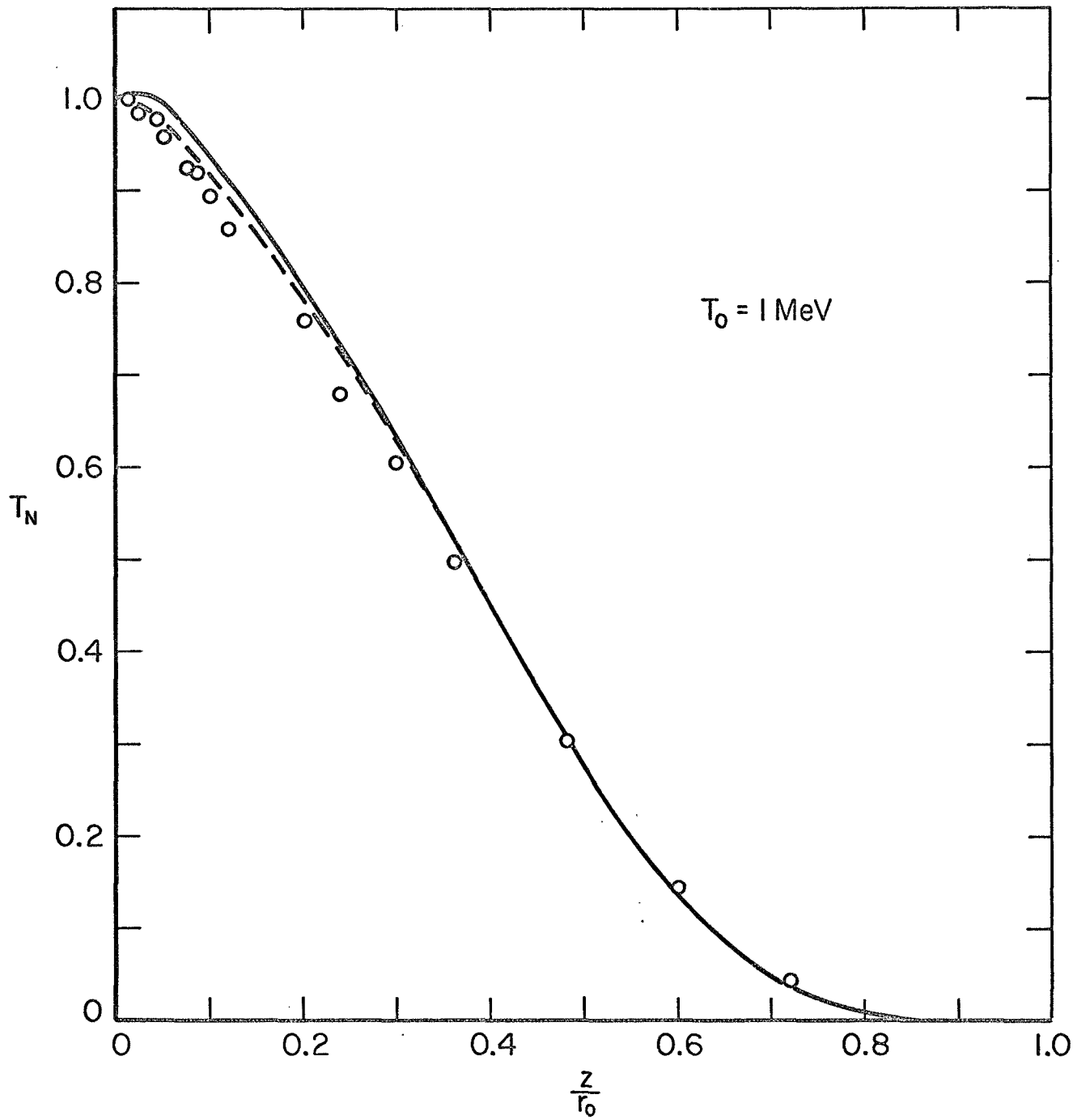

Fig. 5d

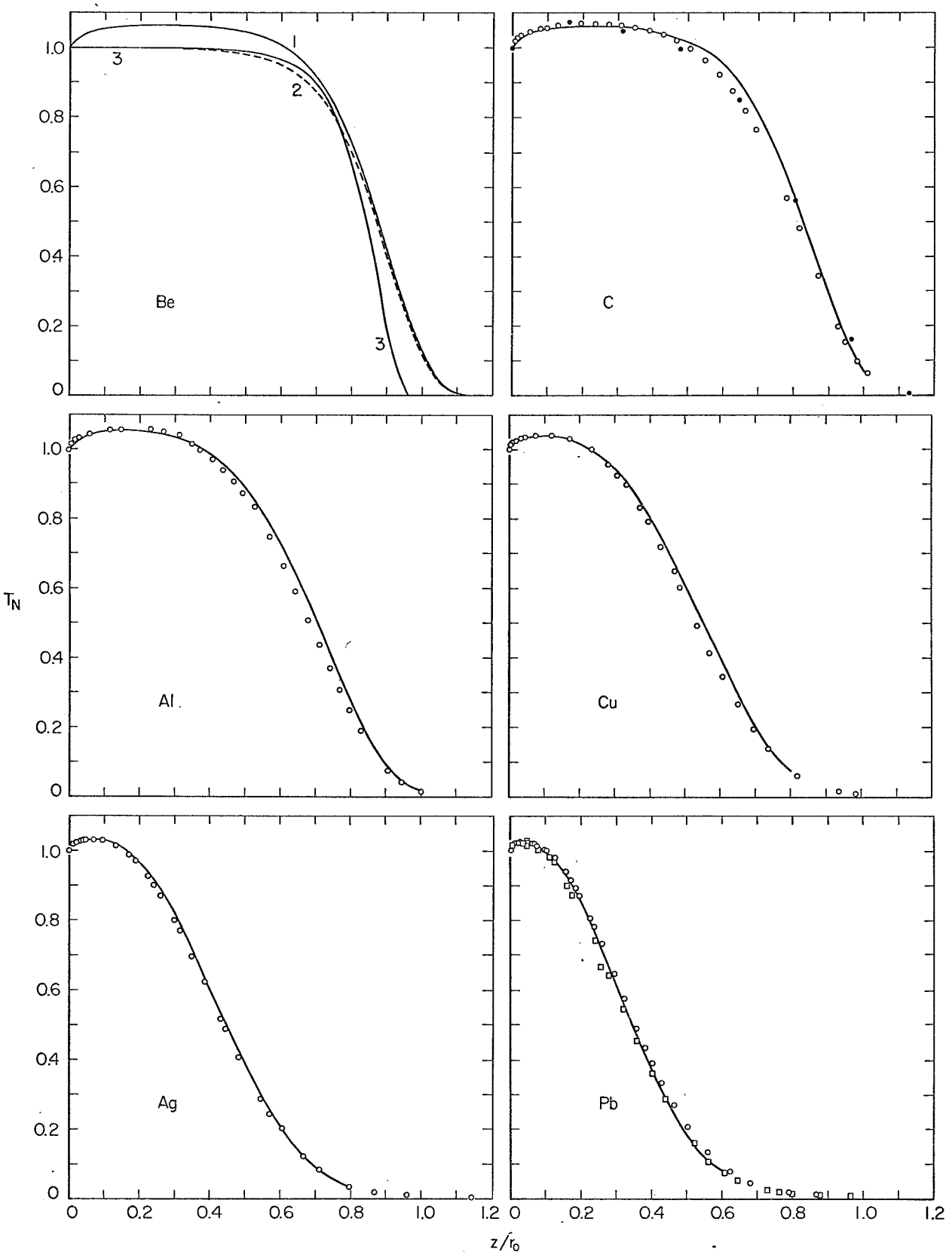

Fig. 6

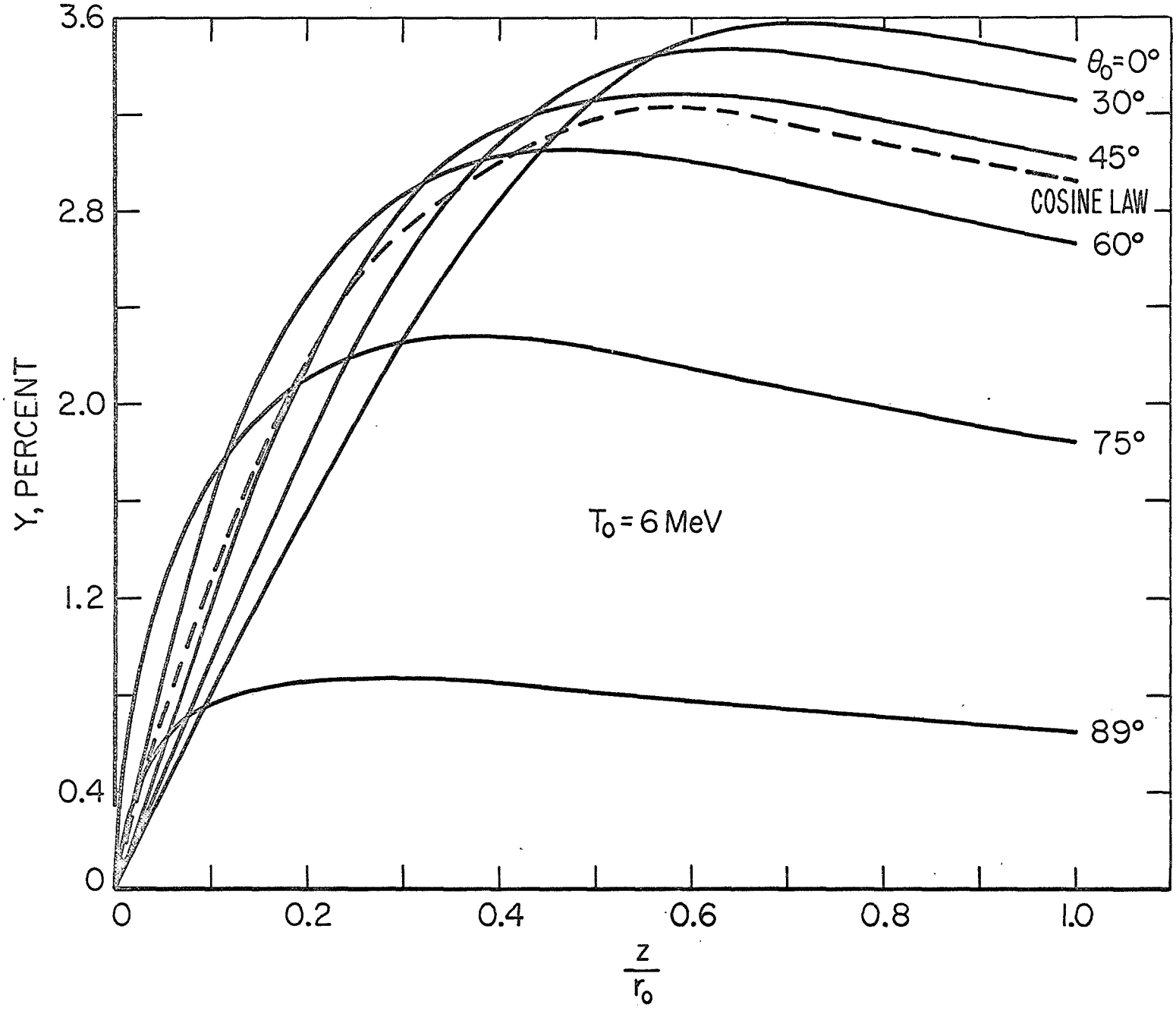
3.6
2.8
2.0
1.2
0.4
0
Y, PERCENT
0
0.2
0.4
0.6
0.8
1.0
z/r0
θ0=0°
30°
45°
COSINE LAW
60°
75°
89°
T0 = 6 MeV

Fig. 7

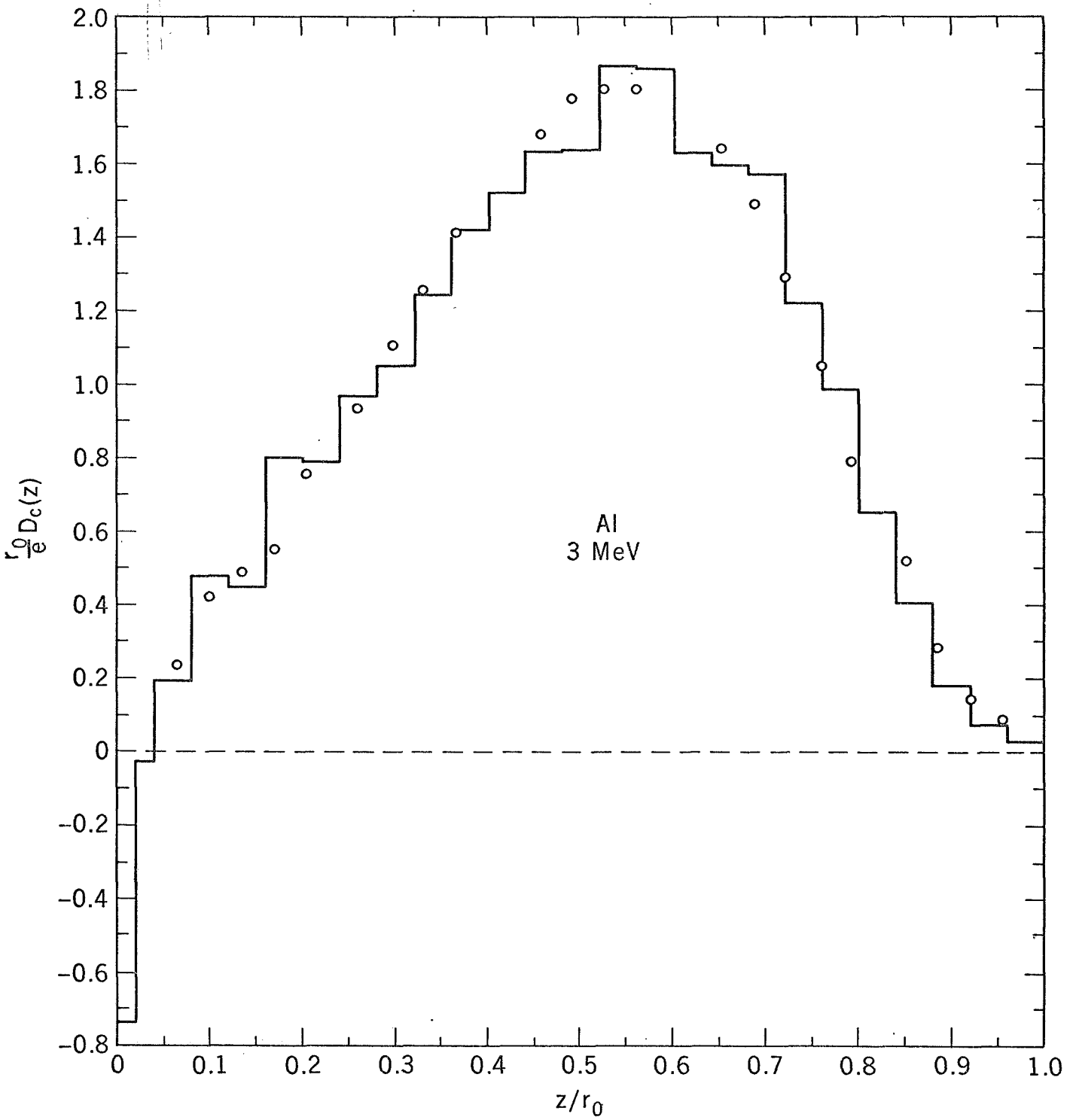
2.0
1.8
1.6
1.4
1.2
1.0
0.8
0.6
0.4
0.2
0
-0.2
-0.4
-0.6
-0.8
$\frac{r_0}{e} D_c(z)$
Al
3 MeV
0
0.1
0.2
0.3
0.4
0.5
0.6
0.7
0.8
0.9
1.0
z/r_0

Fig. 8a

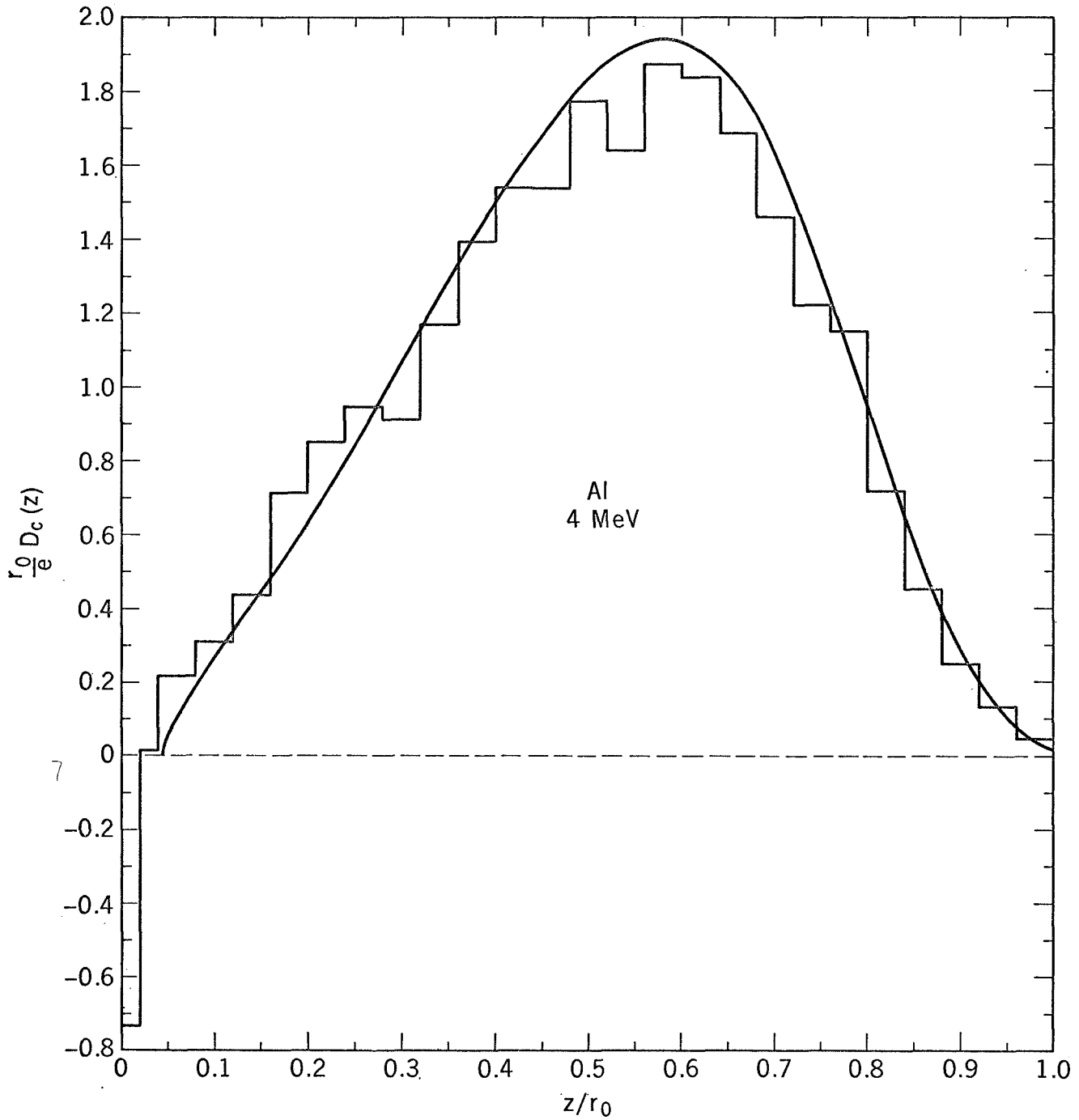
2.0
1.8
1.6
1.4
1.2
1.0
0.8
0.6
0.4
0.2
0
-0.2
-0.4
-0.6
-0.8
$\frac{r_0}{e} D_c(z)$
Al
4 MeV
0
0.1
0.2
0.3
0.4
0.5
0.6
0.7
0.8
0.9
1.0
z/r_0

Fig. 8b

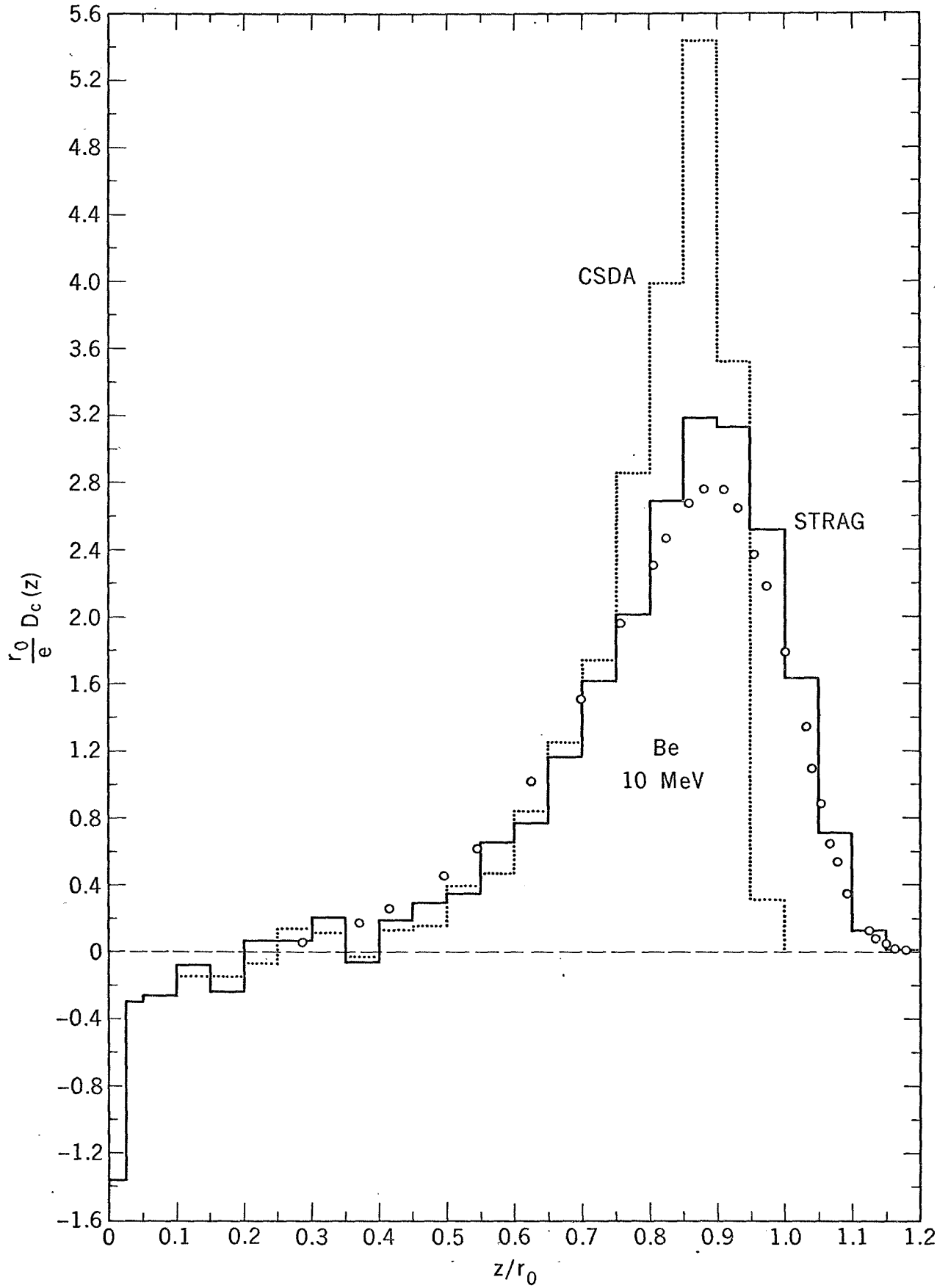
CSDA
STRAG
Be
10 MeV
$\frac{r_0}{e} D_c(z)$
z/r_0
5.6
5.2
4.8
4.4
4.0
3.6
3.2
2.8
2.4
2.0
1.6
1.2
0.8
0.4
0
-0.4
-0.8
-1.2
-1.6
0
0.1
0.2
0.3
0.4
0.5
0.6
0.7
0.8
0.9
1.0
1.1
1.2

Fig. 8c

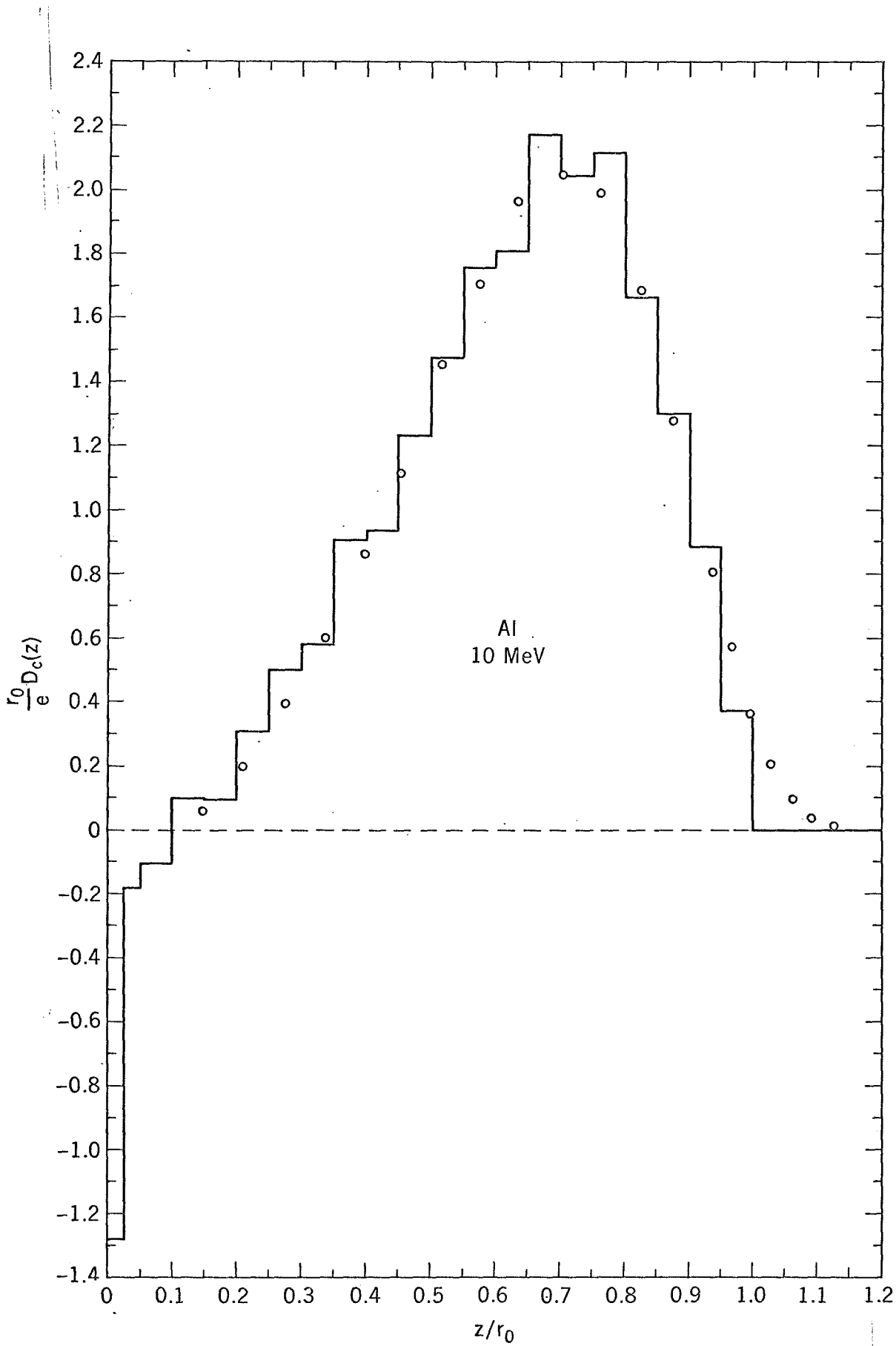
Al
10 MeV
$\frac{r_0}{e} D_c(z)$
z/r_0
2.4
2.2
2.0
1.8
1.6
1.4
1.2
1.0
0.8
0.6
0.4
0.2
0
-0.2
-0.4
-0.6
-0.8
-1.0
-1.2
-1.4
0
0.1
0.2
0.3
0.4
0.5
0.6
0.7
0.8
0.9
1.0
1.1
1.2

Fig. 8d

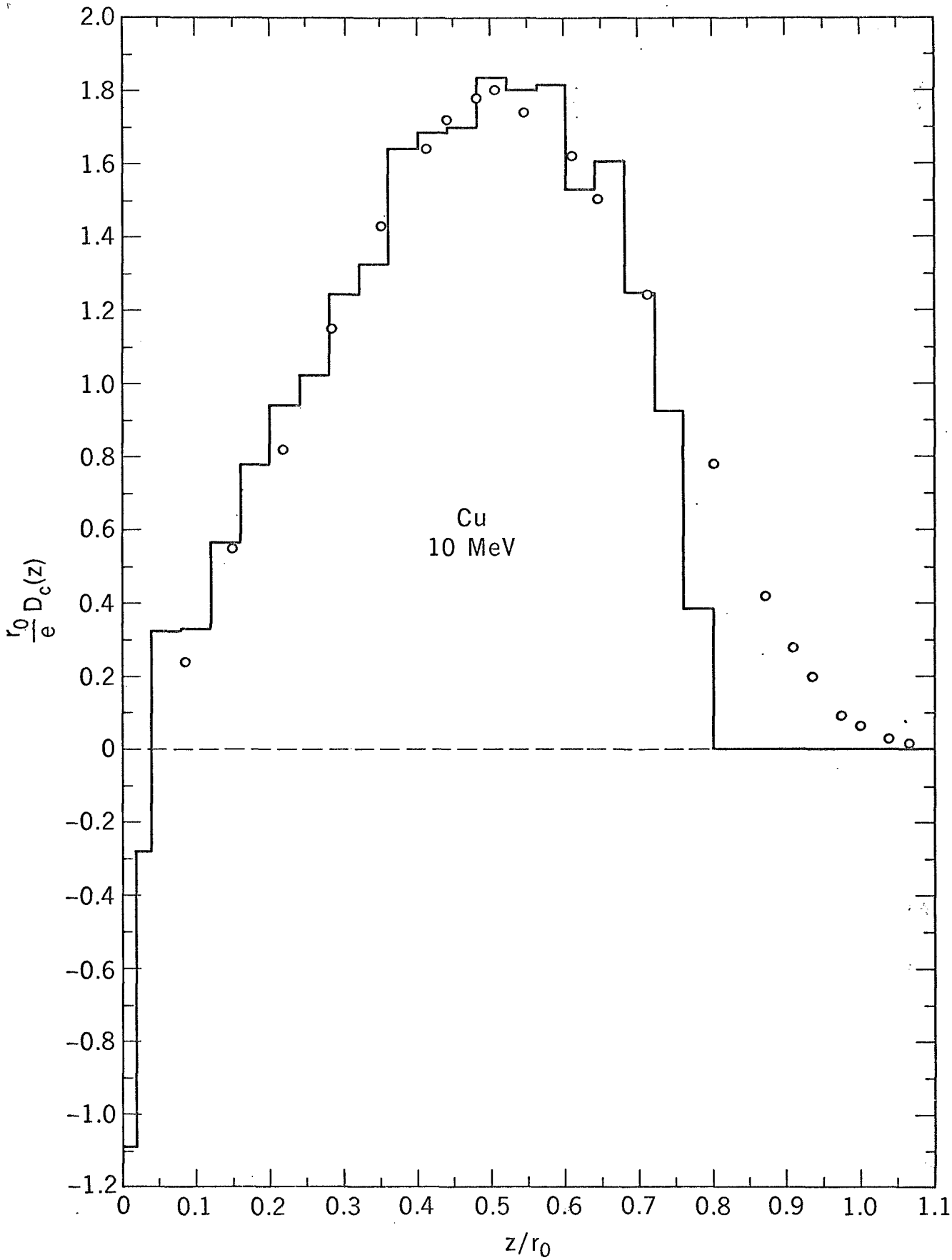
Cu
10 MeV
$\frac{r_0}{e} D_c(z)$
z/r_0
2.0
1.8
1.6
1.4
1.2
1.0
0.8
0.6
0.4
0.2
0
-0.2
-0.4
-0.6
-0.8
-1.0
-1.2
0
0.1
0.2
0.3
0.4
0.5
0.6
0.7
0.8
0.9
1.0
1.1

Fig. 8e

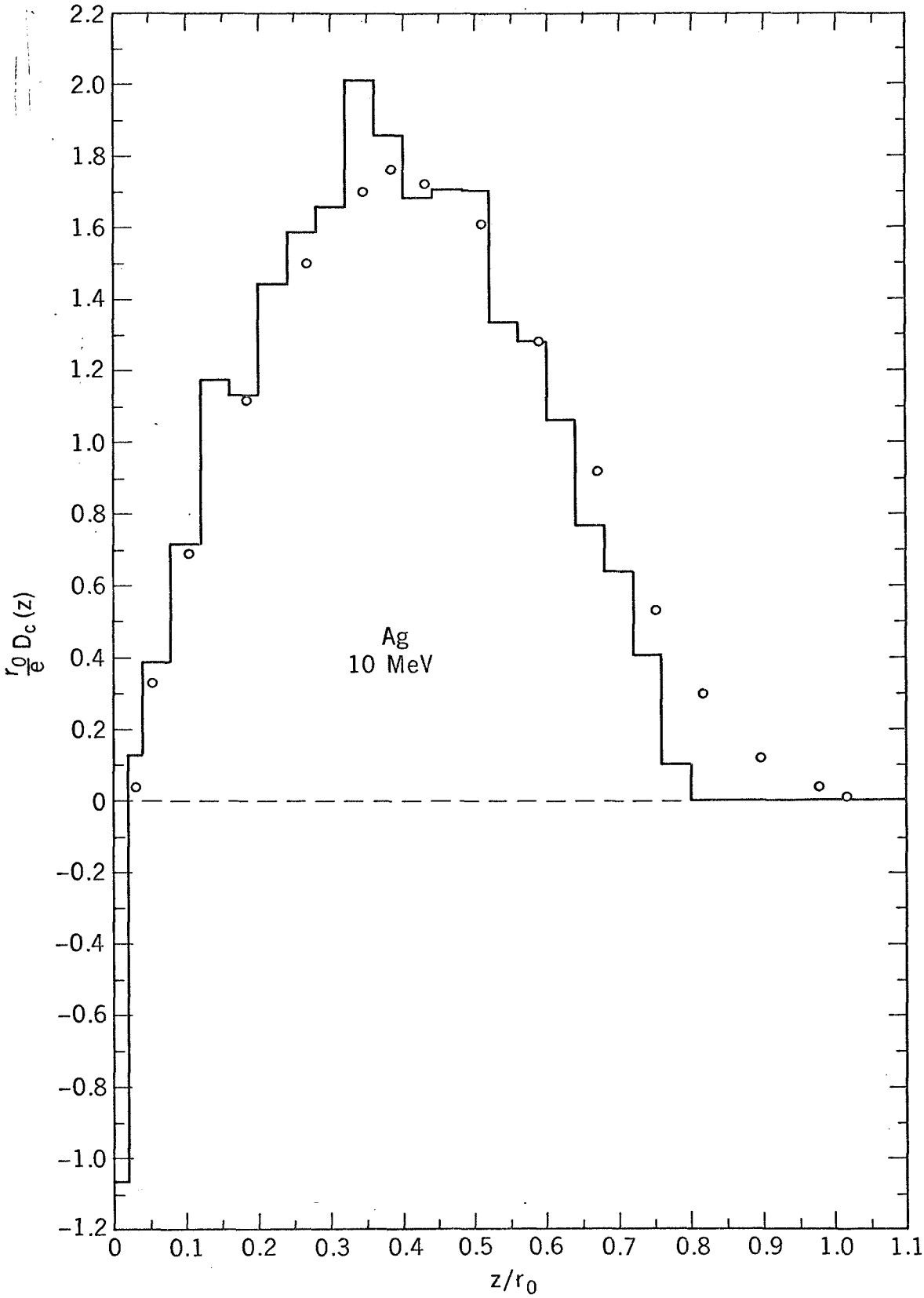
2.2
2.0
1.8
1.6
1.4
1.2
1.0
0.8
0.6
0.4
0.2
0
-0.2
-0.4
-0.6
-0.8
-1.0
-1.2
$\frac{r_0}{e} D_c(z)$
Ag
10 MeV
0
0.1
0.2
0.3
0.4
0.5
0.6
0.7
0.8
0.9
1.0
1.1
z/r_0

Fig. 8f

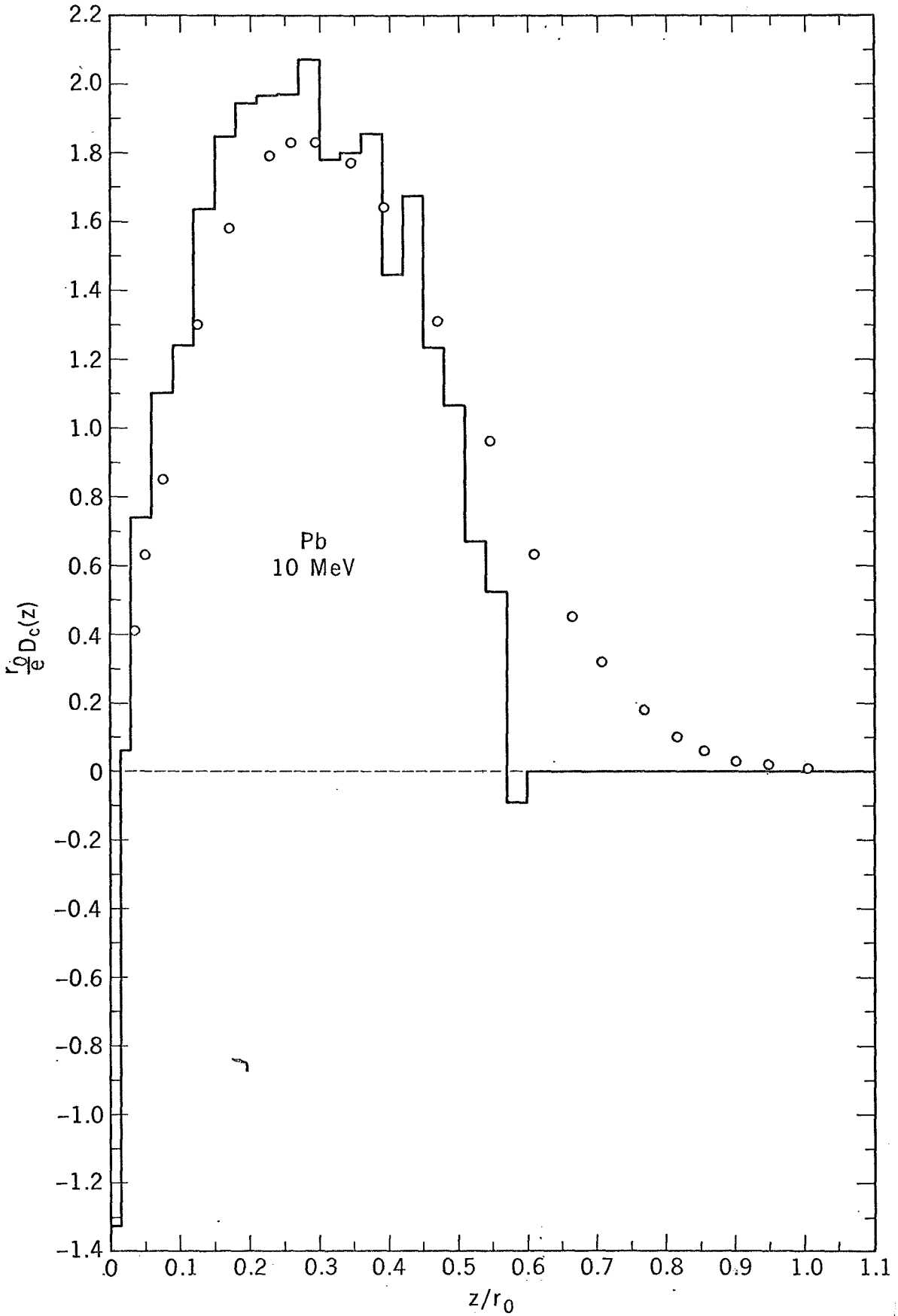
Pb
10 MeV
$\frac{r_0}{e} D_c(z)$
z/r_0
2.2
2.0
1.8
1.6
1.4
1.2
1.0
0.8
0.6
0.4
0.2
0
-0.2
-0.4
-0.6
-0.8
-1.0
-1.2
-1.4
0
0.1
0.2
0.3
0.4
0.5
0.6
0.7
0.8
0.9
1.0
1.1

Fig. 8g

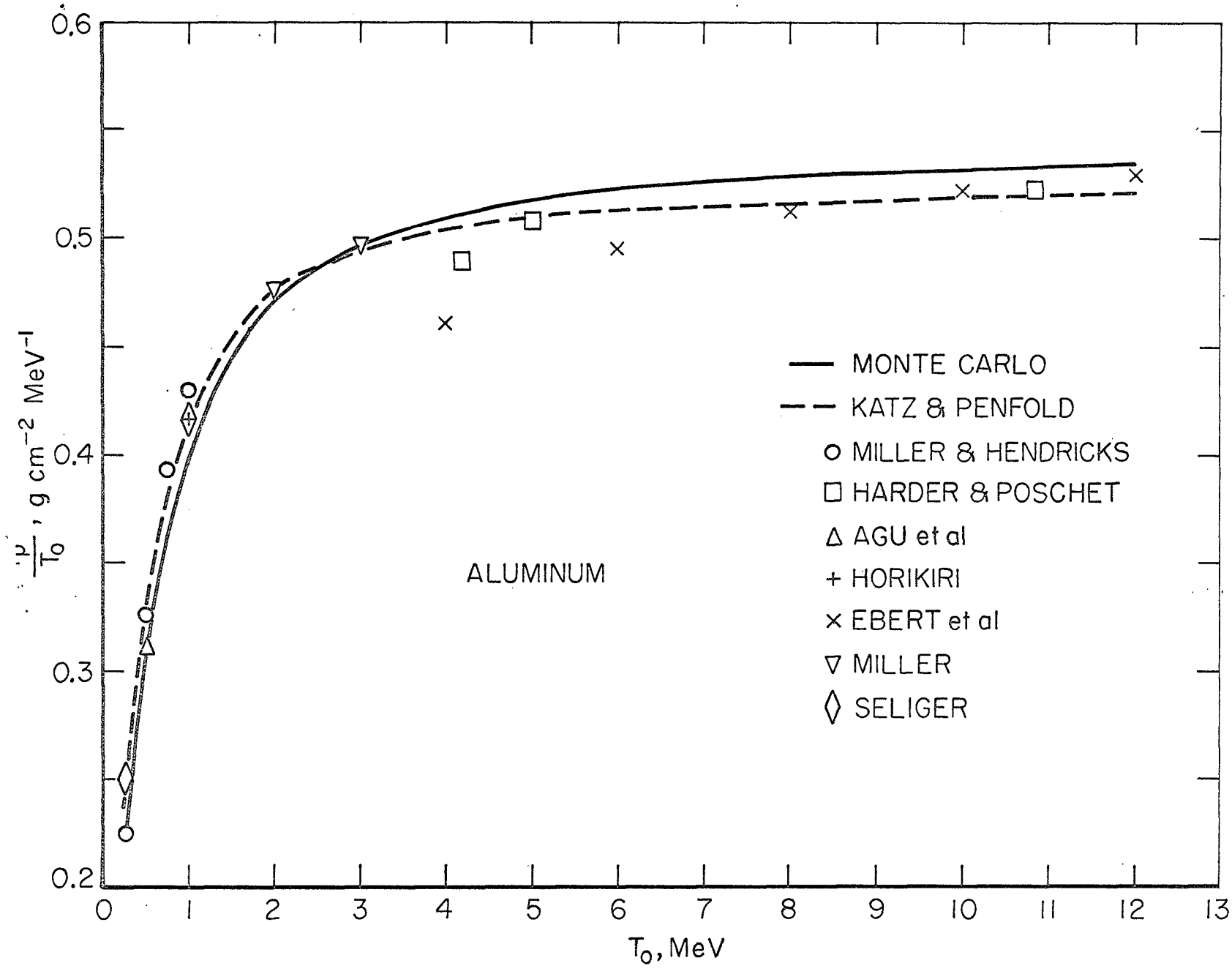
0.6
0.5
0.4
0.3
0.2
$\frac{\mu}{T_0}$, g cm^{-2} MeV^{-1}
0
1
2
3
4
5
6
7
8
9
10
11
12
13
T_0, MeV
ALUMINUM
MONTE CARLO
KATZ & PENFOLD
MILLER & HENDRICKS
HARDER & POSCHET
AGU et al
HORIKIRI
EBERT et al
MILLER
SELIGER

Fig. 9